Feline Coronavirus Infection of Domestic Cats Causes Development of Cross-Reactive Antibodies to SARS-CoV-2 Receptor Binding Domain

Short title: **Cross-Reactive Antibodies to SARS-CoV-2 RBD**

Janet K. Yamamoto[1,2]*, Lekshmi K. Edison[1,2], Dawne K. Rowe-Haas[3], Tomomi Takano[4], Chen Gilor[5], Chiquitha D. Crews[5], Apichai Tuanyok[2,6], Ananta P. Arukha[1,8], Sayaka Shiomitsu[2,6], Heather D.S. Walden[1], Tsutomu Hohdatsu[4], Stephen M. Tompkins[3], John G. Morris Jr[7], Bikash Sahay[2,6], and Subhashinie Kariyawasam[1,2]

[1] Department of Comparative, Diagnostic, and Population Medicine (CDPM), College of Veterinary Medicine, University of Florida, Gainesville, FL 32610

[2] Laboratories of Comparative Immunology & Virology for Companion Animals, CDPM, College of Veterinary Medicine, University of Florida, Gainesville, FL 32610

[3] Center for Vaccines and Immunology, College of Veterinary Medicine, University of Georgia, Athens, GA 30602

[4] Laboratory of Veterinary Infectious Disease, Department of Veterinary Medicine, Kitasato University, Tokyo, Japan 108-8641

[5] Department of Small Animal Clinical Science, College of Veterinary Medicine, University of Florida, Gainesville, FL 32610

[6] Department of Infectious Diseases and Immunology, College of Veterinary Medicine, University of Florida, Gainesville, FL 32610

[7] Emerging Pathogens Institute, University of Florida, Gainesville, FL 32610

[8] Current Address: Department of Neurosurgery, Medical School, University of Minnesota, Minneapolis, MN 55455

* yamamoto@ufl.edu

Abstract (265)

The current study was initiated when our specific pathogen-free laboratory toms developed unexpectedly high levels of cross-reactive antibodies to human SARS-CoV-2 (SCoV2) receptor binding domain (RBD) upon mating with feline coronavirus (FCoV)-positive queens. Multi-sequence alignment analyses of SCoV2 Wuhan RBD and four strains each from FCoV serotypes 1 and 2 (FCoV1, FCoV2) demonstrated amino acid sequence identity of 11.5% and similarity of 31.8% with FCoV1 RBD, as well as 12.2% identity and 36.5% similarity for FCoV2 RBD. The sera from all three toms and three mated queens cross-reacted with SCoV2 RBD and reacted with FCoV1 RBD and FCoV2 spike-2, nucleocapsid, and membrane proteins of FCoV2 whole-virus, but not with FCoV2 RBD. Additionally, the plasma from all six FCoV2-inoculated laboratory cats reacted with FCoV2 and SCoV2 RBDs, but not with FCoV1 RBD. In another study, eight group-housed laboratory cats from a different lineage had a range of serum cross-reactivity to SCoV2 RBD even 15 months later. Such cross-reactivity was also observed in FCoV1-positive group-housed pet cats. The SCoV2 RBD at a high non-toxic dose and FCoV2 RBD at a 60-400-fold lower dose blocked the *in vitro* FCoV2 infection of the feline cells, demonstrating their close structural conformations essential as vaccine immunogens. Furthermore, such cross-reactivity to SCoV2 RBD was also detected by the peripheral blood mononuclear cells of both transient and chronically FCoV1-infected cats. Overall, the cross-reactivity with SCoV2 RBD by the sera from both serotypes of FCoV-infected cats also suggests that the cross-reactive epitope(s) on FCoV1 and FCoV2 RBDs may be similar to those of SCoV2 RBD and provides essential insights to developing a pan-CoV vaccine.

Author Summary (155)

To date, there are no reports on the sera from feline coronavirus (FCoV)-infected cats cross-reacting with either SARS-CoV-1 or SARS-CoV2 (SCoV2) receptor binding domains (RBDs). This report describes the presence of cross-reactive antibodies to SCoV2 RBD in the sera of FCoV-infected laboratory cats, even though SCoV2 RBD and each FCoV serotype (FCoV1, FCoV2) RBD had minimal sequence similarity. However, this observation of serum cross-reactivity to SCoV2 RBD was confirmed by more stringent antibody-based assays and viral assays. Furthermore, both serotypes of FCoV-infected cats, including FCoV1-infected pet cats, produced the cross-reactive antibodies, and such cross-reactivity to SCoV2 RBD was also detected, most likely, by the T cells in peripheral blood mononuclear cells of both transient and chronically FCoV1-infected cats. Since SCoV2 RBD is essential component for current vaccines against COVID-19 disease, our findings should provide essential insights to developing a pan-coronavirus vaccine that induces full-scale immunity to completely prevent SCoV2 infection in humans and pet animals.

Introduction

The global prevalence of feline coronavirus (FCoV) infection ranges from 6.6%-95% in multi-cat households and catteries [1-3]. FCoV is distributed into two phylogenic lineages of serotypes 1 and 2 (FCoV1, FCoV2). Both serotype FCoVs infect predominantly epithelial cells of the gastrointestinal tract and cause a mild gastrointestinal disease (e.g., diarrhea, vomiting, and transient weight loss) in domestic cats, especially in kittens. Often, upon chronic infection, these viruses can also mutate into pathogenic and fatal variants. These variants, called feline infectious peritonitis viruses (FIPVs), infect monocytes and macrophages, spreading throughout the body [4-6]. No known cases of FCoV infection in humans have been reported. However, the FCoV sequence sections have been found in recombinant coronaviruses infecting humans [7-9]. In comparison, many cases of SARS-CoV-2 (SCoV2) infection of pet cats have been reported worldwide through transmission from COVID-19-positive owners to their pet cats. These cats displayed mild symptoms or remained asymptomatic, even when found positive for SCoV2 by RT-PCR [10-12]. Experimental inoculation of laboratory cats with a human isolate of SCoV2 caused infection, ranging from mild to asymptomatic symptoms. These infected cats were diagnosed as RT-PCR positive through nasal and/or fecal swabs [13-15]. SCoV2 transmission from inoculated cats to non-inoculated cats through contact exposure has been demonstrated by multiple research groups worldwide [13,15]. Similarly, transmissions of SCoV2 from COVID-19-positive owners to their symptomatic and asymptomatic pet dogs have been reported [11,12,16]. Experimental infection of laboratory dogs also confirmed that dogs could be infected with SCoV2 [13,14].

Studies have shown that FCoV-infected cats develop antibodies that cross-react with SARS-CoV1 (SCoV1) nucleocapsid [17] but not with SCoV1 spike 1 (S1) glycoprotein [18], where the SCoV1 receptor binding region (RBD) is located [19]. SCoV1

infection in humans was first discovered in November 2002 in a patient with atypical pneumonia in Guangdong, China [20]. By February 2003, this virus was rapidly transmitted to a large population in Hong Kong, causing severe acute respiratory syndrome (SARS). The intermediate host for SCoV1 was suspected to be a masked palm civet [21]. SCoV1 preparation isolated from a patient, was inoculated intratracheally into six laboratory cats. This resulted in asymptomatic infection in all four cats, based on positive virus isolation and viral RT-PCR of the pharynx, trachea, and lungs [22]. Furthermore, two non-inoculated cats housed together with the SCoV1 inoculated cats became PCR positive starting day 2 of contact exposure with a peak titer at day 6. By day 28, they had seroconverted with a virus-neutralizing antibody (NAb) titer of 40 and 160. One pet cat living in an apartment block with over 100 residents positive for SCoV1 was also positive for SCoV1 infection [22].

Both SCoV1 and SCoV2 belong to genus Betacoronavirus of family Coronaviridae, while FCoV1 and FCoV2 belong to genus Alphacoronavirus based on phylogenetic analyses [23]. Both SCoV1 and SCoV2 RBDs bind with human angiotensin converting enzyme-2 (hACE2) to infect hACE2-expressing human cells and serving as the major target of the NAbs generated by the infected hosts [24]. In contrast, neither FCoV1 nor FCoV2 use ACE2 as their host cell receptor [25,26]. The cell receptors for FCoV2 and canine coronavirus serotype 2 (CCoV2) are reported to be feline and canine aminopeptidase-N (fAPN and cAPN), respectively, which is like the human cold Alphacoronavirus (HCCoV) 229E, using human APN (hAPN) as its primary cell receptor [25,27,28]. The cell receptor for FCoV1 is still unknown and this is complicated by the fact that FCoV1 isolates do not readily replicate in cell cultures [6,29]. FCoV1 infection is more prevalent worldwide, including the US, while the FCoV2 infection is found predominantly in Southeast Asia [1-3,6,30]. FCoV2 is reported to be a recombinant FCoV1 backbone

with CCoV2 spike (S) glycoprotein [29,31]. Since hACE2 is the major cell receptor for SCoV2, SCoV2 infections of cats and dogs are reported to be mediated by the feline ACE2 (fACE2) and canine ACE2 (cACE2), respectively, based on their amino acid (aa) sequence similarity of fACE2 and cACE2 to hACE2 and the binding analyses of SCoV2 to species-specific ACE2 [23,24,32,33].

The aa sequence comparison between SCoV1 and SCoV2 S proteins demonstrates a considerably high sequence identity of 76%, and their RBDs similarly show a high sequence identity of 73% [34-36]. Hence, the aa sequence similarity should be much higher. Since the sera from FCoV1 and FCoV2 infected cats cross-react with SCoV1 nucleocapsid but not with SCoV1 S1 glycoprotein [17,18], it can be inferred from those reports that sera from FCoV1 and FCoV2 infected cats can cross-react with SCoV2 nucleocapsid but not with SCoV2 S1 glycoprotein, and, consequently, not with the SCoV2 RBD which resides on S1 glycoprotein. Furthermore, a few aa sequence analysis studies demonstrate that the Wuhan SCoV2 S glycoprotein is distinctly different from S glycoproteins of FCoV1 and FCoV2 [23,31]. The location for FCoV1 and FCoV2 RBDs has yet to be determined by biological analysis, but it has recently been predicted to be around residues 526-676, based on RBD sequence locations of porcine enteric diarrhea virus (PEDV) RBD at B residues 510-640 and transmissible gastrointestinal enteric virus (TGEV) RBD at D3 residues 500-651 [37-39]. The TGEV RBD has been reported to bind to the porcine APN as its primary host cell receptor [27,39], but whether PEDV RBD binds to pAPN as its host cell receptor is still controversial [38,40]. The RBD sequence prediction of both PEDV and TGEV was based on monoclonal Ab (MAb) studies, identifying the most potent neutralizing MAb(s) to these porcine Alphacoronaviruses reacting to B and D3 residue regions, respectively [38,39]. Although neutralizing MAb (nMAb) studies have been performed against FCoV2 [41,42], the location and the native

conformation of FCoV1 and FCoV2 RBDs have yet to be clearly defined and confirmed by biological analyses required for use as vaccine immunogens.

Our laboratory has recently discovered that, shortly after specific pathogen-free (SPF) toms mated with FCoV-positive queens, they developed minor episode(s) of diarrhea with only low production of FCoV antibodies (Abs) but unexpectedly high levels of cross-reactive Abs to human SCoV2 RBD. Consequently, as a confirmation of the original finding, these sera from FCoV infected cats were tested for their cross-reactivity to SCoV2 RBD by more stringent ELISA, immunoblot analyses, SCoV2 RBD blocking assay, and SCoV2 RBD stimulation of peripheral blood mononuclear cells (PBMC). Lastly, we further characterized the nature of FCoV transmission in cats at inducing cross-reacting Abs to SCoV2 RBD.

Results

Initial serological studies in FCoV naturally infected laboratory cats

FCoV whole-virus (WV) ELISA and SCoV2 ELISA with overnight serum incubation: Our studies on FCoV were initiated when four laboratory queens donated by the University of Georgia (UGA) were mated with three SPF inbred toms from our laboratory at the University of Florida (UF) (Fig 1A). The four juvenile laboratory cats born from two UGA queens (UGAQ3, UGAQ4) had FCoV Abs at 12 and 16 weeks of age based on FCoV2-WV ELISA. The UGA queens were all seropositive for FCoV2 (Fig 1B), and the sera from the toms, after mating, were weakly seropositive for FCoV2 but had no neutralizing Abs (NAbs) to FCoV2 (Fig 1B). Since these juvenile cats were to be used for a SCoV2 inoculation study at UGA, their serum was collected before shipment to UGA and tested by SCoV2 RBD ELISA. Three of the four juvenile cats had a serum that cross-reacted moderately with the SCoV2 RBD (Fig 1C).

Stringent FCoV-WV ELISA and SCoV2 RBD ELISA: The sera from all four UGA queens and three toms were incubated at the same dilution for only one hour instead of overnight, and PBS was used instead of bicarbonate buffer for coating of the antigen on the ELISA plate. In addition, ELISA with bovine serum albumin (BSA) antigen was included since the UGA queens were vaccinated three years ago with commercial vaccines. The veterinary vaccines were often contaminated with BSA. This BSA control was also important because the FCoV2-WV preparation contained about 5% BSA, whereas the RBDs were highly purified and devoid of BSA. Two UGA queens (UGAQ1, UGAQ4) had high levels of serum reactivity with FCoV but without any reactivity with BSA and SCoV2 RBDs, while the other two queens (UGAQ2, UGAQ3) had high serum reactivities with FCoV, which were slightly higher than the serum reactivities with BSA (Fig 1D). The sera from UGAQ2 also had substantial cross-reactivities with both SCoV2 RBDs (UF and MassBiologics (MB) RBDs) (S1A Fig), whereas the sera from UGAQ3 had a modest cross-reactivity with MB-RBD and below the threshold cross-reactivity with UF-RBD. All UGA queens were group housed together upon arrival on Oct. 25, 2019. The earliest serum collected from the queens was on Dec. 19, 2019 from UGAQ1 (Fig 1D). Hence, they were most likely infected with FCoV, instead of SCoV2 and not from contact with a COVID-19-positive animal caretaker, since the first case of COVID-19 in Florida was reported on March 2, 2022 [43]. The serum collected from 5HQT1 on Jan. 29, 2020 (Fig 1E*;* Post-2 mo) cross-reacting with SCoV2 RBD supports FCoV infection, based on the date of the first Florida cases.

As expected, the sera from all toms before mating had no reactivity with FCoV, both UF/MB-RBDs (Fig 1E), and BSA (S1B Fig). However, post-mating sera from all toms had significant reactivity with SCoV2 RBDs but not with FCoV, compared to the corresponding pre-mating control results. The highest titers to SCoV2 RBDs were

observed at the earliest timepoint of serum collection closest to the first exposure to the FCoV-positive queen. Subsequent sera showed declines that were still significantly different from the pre-serum titers (p<0.05; pre- and post-exposure paired T-test). The decline suggested that the development of cross-reactive Abs to SCoV2 RBD could have occurred during active FCoV infection. A slight conflict was observed between the substantial reactivity with FCoV for the toms (Fig 1B) and no reactivity with FCoV for the toms (Fig 1E). This may be due to the technical difference as detailed above. Overall, the stringent ELISA confirmed the sera from all three toms cross-reacted strongly with SCoV2 RBD. Only one long-term FCoV-infected queen UGAQ2 also had a high titer of cross-reactive Abs to SCoV2 RBD (Fig 1D).

The lack of S1 and RBD aa sequence identity/similarity between SCoV2 and FCoVs

Sequence analyses of SCoV2 and FCoV structural proteins: The aa sequence comparison between Wuhan SCoV2 *versus* FCoV1 and between SCoV2 *versus* FCoV2 demonstrated SCoV2 structural proteins (spike, envelope, membrane) were shorter than FCoV1 and FCoV2, with the exception of nucleocapsid protein and S2 (S2A Fig). The least aa identity and similarity were observed between SCoV2 and FCoV1/FCoV2 at the S1 glycoprotein among the five structural proteins composing these viruses. The aa sequence identity and similarity between S1 glycoproteins of SCoV2 and FCoV1 had 13.0% and 40%, respectively, whereas, between SCoV2 and FCoV2, 16.3% and 43.4%. When comparing the cleavage sites separating S1/S2 among SCoV2, FCoV1 and FCoV2, SCoV2 S1/S2 cleavage site appears closer to the FCoV1 S1/S2 cleavage site than that of FCoV2 [44,45]. In contrast, the S2 glycoprotein between SCoV2 and FCoV1/FCoV2 had the highest aa identity of 30.0% and 33.5% with the second highest similarity of 62.2% and 64.5%, respectively, among all structural proteins. Hence, S1

glycoprotein was the most distinctly different structural protein between SCoV2 and FCoV1/FCoV2 among all five structural proteins.

When FCoV1 and FCoV2 spike glycoprotein sequences were compared, the S1 glycoprotein sequence had 29.5% and 31.6% identity and 62.9% and 64.5% similarity, which were much lower than the S2 sequence that had 60.6% and 68.7% identity and 84.0% and 89.9% similarity (S2A Fig). The S1/S2 cleavage site for the FCoV2 is proposed to be at the S2' cleavage site (another cleavage site on S2 glycoprotein) next to the fusion peptide because S1/S2 cleavage motif is absent in the location usually observed for FCoV1 and other coronaviruses [44-46]. Note that most coronaviruses, including SCoV2 and FCoV1, have the S2' cleavage site, but, for brevity, only S1/S2 cleavage site results were used in our analysis. The difference in the aa sequence between FCoV1 and FCoV2 at the envelope (Env), NC, and M ranged from 92.8%-96.3% identity and 97.6%-98.5% similarity, which demonstrated the high conservation between FCoV1 and FCoV2 for those structural proteins. The molecular weight (MW) of the structure proteins without glycosylation was predicted (S2B Fig) to analyze FCoV2-WV immunoblot described later.

Sequence analyses of SCoV2 and FCoV RBDs: Next, the Wuhan RBDs of UF and MB were aligned with four known FCoV1 S1 sequences and another set with four known FCoV2 S1 sequences using Clustal O (1.2.1) multiple sequence alignment of JustBio alignment server (https://justbio.com/) (Fig 2A and 2B). The goal of this alignment analysis was to identify the potential FCoV1 and FCoV2 RBD sites for use as the vaccine immunogens. Our logic for using such a comparison is based on the fact that species-specific ACE2 is used by SCoV2 to infect cats, dogs, and humans. The Wuhan SCoV2 RBD sequence is distinctly different in aa sequence from the RBD sequences of FCoV1 (11.5% & 12.3% identity; 31.8% & 33.6% similarity) and FCoV2 (12.2% & 12.3% identity;

36.5% & 37.7% similarity) (Fig 2C). The first value is based on UF-RBD, and the second value is based on MB-RBD. As shown, the carboxyl-end of the UF-RBD sequence (residues 319-529) is shorter by 12 aa from the MB-RBD sequence (aa residues 319-541) (Fig 2A and 2B and S1A Fig). The FCoV2 RBD had slightly more aa similarity with the Wuhan SCoV2 UF- and MB-RBDs than those between the FCoV1 RBD and SCoV2 RBDs (Fig 2C). Thus, the aa sequences of the two FCoV2 RBDs (36.5% and 37.7%), more than the two FCoV1 RBDs (31.8% and 33.6%), had slightly more similarity to SCoV2 UF- and MB-RBD sequences.

The full-length aa sequence comparison of S glycoproteins of the SCoV2 Wuhan strain and FCoV2 79-1146 strain displays the S1/S2 cleavage site for SCoV2 at a location different from the S1/S2 cleavage site for FCoV2 (S3A Fig) [36,44,45]. In addition, the SCoV2 RBD sequence alignment pattern with a single FCoV2 RBD sequence of the full-length S protein sequence differs slightly from the one aligned with four FCoV2 RBD sequences (Fig 2B), even though both analyses used the JustBio alignment server. The full-length S sequences between SCoV2 and FCoV2 show the RBD has the least sequence similarity followed by the N-terminal domain (NTD) and then C-terminal domain (CTD) with the most similarity or conservation among two S1 domains (S3B Fig). This pattern was the same whether the S1/S2 cleavage site for SCoV2 or FCoV2 was used. Furthermore, S2 sequence had the most aa sequence conservation between SCoV2 Wuhan and FCoV2 79-1146.

The full-length S sequences of FCoV1 UCD-1 strain were compared to the S sequence of the SCoV2 Wuhan strain and showed major changes in gap location on the SCoV2 sequence when compared to the single FCoV1 sequence (S4A Fig) or to the four FCoV1 sequences (Fig. 2*A*). The S1/S2 cleavage site for SCoV2 is only 46 aa plus five gaps away from the counterpart S1/S2 cleavage site for FCoV1 (S4A Fig) [36,44].

Conversely, the FCoV1 S1/S2 cleavage site is 37 aa plus 14 gaps from the counterpart SCoV2 cleavage site [45]. Thus, the S1/S2 cleavage sites are closer to SCoV2 and FCoV1 than those between SCoV2 and FCoV2. The most aa sequence conservation is observed at the S2 sequence, followed by S1 CTD, S1 NTD, and S1 RBD, which is identical to those observed between SCoV2 and FCoV2.

The comparison of the proposed FCoV1 and FCoV2 RBDs show three major gaps from the mid-to-carboxyl-end, which overlaps our predicted receptor binding motif (RBM), and has only 27.3% aa identity and 62.5% aa similarity (Fig 2D and 2E). The FCoV1 and FCoV2 at the proximity to our RBMs are quite different which may explain why FCoV1 does not use fAPN as a host cell receptor. The aa mutation sites that lower or eliminate the neutralization activity of the reported six nMAbs are shown with three color-coded symbols for each nMAb below the FCoV2 RBD sequence (Fig 2D). The aa mutation sites are clustered at mid-to-carboxyl-end of our proposed RBD which indicate that FCoV2 neutralizing epitopes are at or in the proximity of our proposed RBM.

Immunoblot analyses of sera from queens and toms

The proposed FCoV2 RBD, with the most cross-reactive sectional regions overlapping with SCoV2 RBD, as highlighted in the magenta sequence (Fig 2B), were 1) produced in the same cell expression system with the same plasmid, 2) purified similarly as SCoV2 UF-RBD in PBS, and 3) used to develop the immunoblot strips. Two sera (UGAQ2, UGAQ4) from the four queens and the serum from all three toms strongly cross-reacted with the SCoV2 UF-RBD (Fig 3A), but none of them reacted with FCoV2 RBD (Fig 3B). All sera from the queens reacted with FCoV2-WV immunoblot strips strongly at the M (28-32kDa), NC (43kDa), degraded spike S (100-125kDa), and entire spike S (190kDa) (Fig 3C), with weaker bands at 20kDa, 22kDa, 40kDa, and 55kDa except for UGAQ1. The

single serum available from UGAQ1 was collected when she was severely sick from uteritis and on antibiotics. Her serum only reacted to FCoV2-WV at 90kDa and higher (Fig 3C) but not to SCoV2 (Fig 3A), FCoV2 (Fig 3B), and FCoV1 (Fig 3D) RBDs. The toms had reactivity to NC, M, and proteins at 10kDa, 20kDa and 22kDa but almost no reactivity to FCoV2-WV S proteins and degraded S glycoproteins above 90kDa. The same sera from the toms did not react to FCoV2 RBD except for one tom (HOGT3), which reacted weakly with FCoV2 RBD (Fig 3B) and without FCoV2 NAb titer (Fig 1B) but strongly with FCoV1 RBD (Fig 3D). These results demonstrate that the serum from three UGA queens (UGAQ2, UGAQ3, UGAQ4) and all three toms reacted with FCoV1 RBD (Fig 3D). The nil-to-weak cross-reactivity to FCoV2 RBD and strong reactivity to FCoV1 RBD suggest that our toms and queens were infected with FCoV1 which is the most common serotype in the US. Their sera also had nil-to-minimum titers of FCoV2 NAbs (Fig 1B) which further supports our theory of FCoV1 infection of our queens and toms. One serum from a UGA cat (UGA1.4) (Fig 3B) with FCoV2 NAb titer of 378 was our weak control serum that reacted to the FCoV2 RBD.

Characterization of Abs to SCoV2 RBD

Only sera from UGAQ2, UGAQ4 (10 months post-arrival) and all three toms had strong cross-reactivity to SCoV2 RBD (Fig 3A). Both 5HQT1 and HOGT3 were exposed to two FCoV-positive ($FCoV^+$) queens over two breeding cycles (Fig 1A), whereas HOJT2 was exposed to three different $FCoV^+$ queens and retained the strongest SCoV2 RBD reactivity even at 13 months post-first exposure to the first $FCoV^+$ queen (Fig 3A). This observation suggested that this tom was actively producing SCoV2 RBD cross-reactive Abs perhaps by sequential exposure to multiple $FCoV^+$ queens. The queen UGAQ4 was exposed to three different $FCoV^+$ toms during the three breeding cycles (Fig 1A) and had

a moderate reactivity to SCoV2 RBD at 10 months post-first exposure (HOJT2), which was also 3 months post-second exposure (5HQT1) (Fig 3A). Nevertheless, UGAQ4 did not retain the cross-reactive Abs to SCoV2 RBD even after the third exposure to the $FCoV^+$ tom (HOGT3) 13 months post-first exposure (Fig 3A). This observation may suggest that the $FCoV^+$ toms, upon exposure to $FCoV^+$ queens, developed only low titers of FCoV infection based on the low reactivity of their FCoV2-WV Abs and nil-to-negligible serum reactivity to the bands above the predicted FCoV2 S2 band of 80-90 kDa (Fig 3C and 3E2). The rabbit polyclonal Abs to SCoV2 S protein and to S2 protein, but not to S1 protein, cross-reacted with FCoV2 S2, degraded S, and S glycoproteins on FCoV2-WV immunoblot (Fig 3E1). These results confirmed the FCoV2 S, degraded S, and S2 MWs are detected by the sera from most UGAQ cats (Fig 3C and 3E2). Thus, the sera from the three toms with strong cross-reactive Abs to SCoV2 RBD and negligible Abs to FCoV2 S and degraded S may suggest low FCoV1 infection in the toms and the possibility of cross-reactive SCoV2 RBD Abs in lowering their level of FCoV1 infection.

Determining the FCoV2 infection blocking activity of FCoV2 RBD

If the proposed FCoV2 RBD is indeed the RBD site for FCoV2, our FCoV2 RBD should be able to block the FCoV2 infection of the feline cell line (Fc9 cells). The duplicate wells, starting at 2.86 µg/mL, were serially diluted three-fold for each well, up to the titer of 0.106 µg/mL (fourth duplicate wells) and presented <50% cytopathic effect (CPE), whereas all wells for virus control had 100% CPE including the PBS controls (Fig 4A). Thus, 1 $TCID_{50}$ titer, the titer with 50% CPE, is between 0.035-0.106 µg/mL. Another assay demonstrated 1 $TCID_{50}$ titer of 50% blocking observed at about 0.100 µg/mL of FCoV2 RBD (Fig 4B). The SCoV2 RBD at 64.2 µg/mL blocked 100% of FCoV2 infection (first duplicate wells), whereas 42.8 µg/mL blocked 30% CPE. Both FCoV2 and SCoV2 RBDs caused no

cellular toxicity (Fig 4C). Overall, 0.1-1.0 μg/mL of FCoV2 RBD blocked 50%-100% of FCoV2 infection, respectively; whereas 48-64 μg/mL of SCoV2 RBD cross-blocked 50%-100% of FCoV2 infection, respectively, at doses without any cellular toxicity. Hence, the proposed FCoV2 RBD sequence includes the RBD site for FCoV2 infection.

Differential reactivity to the FCoV1 and FCoV2 RBDs of the plasma from the FCoV1 KU-2 and FCoV2 79-1146 inoculated laboratory cats

All plasma from SPF cats inoculated with either FCoV1 KU-2 or FCoV2 79-1146 reacted to FCoV2-WV at NC, M, and S2 (Fig 4D). All plasma from cats inoculated with FCoV1 KU-2 strain strongly reacted with FCoV1 UCD1 RBD (Fig 4E) but not with FCoV2 79-1146 RBD (Fig 4F). As expected, all plasma of cats inoculated with FCoV2 79-1146 strain strongly reacted with homologous FCoV2 79-1146 RBD (Fig 4F) but not with heterologous serotype FCoV1 UCD-1 RBD (Fig 4E). Since the majority of the FCoV1 transmitted cats developed cross-reactive Abs to SCoV2 RBD (Fig 3A), the fact that none of the plasma from FCoV1 KU-2 infected cats cross-reacted with SCoV2 RBD was unexpected (Fig 4G).

The role of feline genetics and group-housing in inducing cross-reactive SCoV2 RBD Abs

Eight laboratory cats living together in group housing were all seropositive for FCoV infection by ELISA and immunoblot analyses (S5A and S5B Fig). Since these cats share the litter pans and FCoV transmits by oral-fecal route [6,29,47], once the immunity to the first infection subsides, they can be susceptible to reinfection at different times based on the immune constitution of the cat. Cat G-2, with the highest FCoV Ab titer, had the strongest cross-reactive Abs to SCoV2 UF-RBD immunoblot, followed by cats G-1, G-5,

and G-7, with modest reactivity to SCoV2 RBD (S5B1 Fig). The remaining cats, G-4 and G-6, had negligible-to-no reactivity during the study, and cat G-3 showed no reactivity initially but 15 months later developed strong cross-reactivity to SCoV2 RBD. All eight cats were negative for FCoV2 RBD Abs throughout the study (S5B2 Fig), but all sera were positive at NC, M, and S2 protein bands by FCoV2-WV immunoblot eventually by 15 months of group-housing (S5B3 Fig). They appear to be all infected with FCoV1 based on lack of reactivity to FCoV2 RBD (S5B2 Fig) and strong reactivity to FCoV1 RBD (S5B4 Fig). In our preliminary findings of group-housed pet cats, all three cats tested were Ab positive for FCoV by FCoV2-WV immunoblot (S5C1 Fig) and for FCoV1 by FCoV1 RBD immunoblot, while being negative for FCoV2 RBD (S5C2 Fig). Remarkably, two of them (KM1, KY at first and second bleeding 2.5 months later) were also positive for SCoV2 RBD.

Interferon-gamma (IFNγ) mRNA production of PBMC from FCoV1-infected cats upon stimulation with SCoV2, FCoV1, or FCoV2 RBD

The PBMC from a transiently FCoV1-infected cat (4GC) and chronically FCoV1-infected cat (G-3) from group-housed laboratory cats referenced above, developed substantial level of IFNγ mRNAs in response to SCoV2 RBD stimulation (Fig 4H). The levels were close to those stimulated by T-cell mitogen (concanavalin A, ConA). Chronically infected cat G-3 also responded with slightly lower, but substantial, IFNγ mRNA level in response to FCoV1 RBD stimulation, whereas transiently infected cat 4GC had no response to FCoV1 RBD. Both infected cats had no response to FCoV2 RBD stimulation. As expected, the PBMC from two uninfected SPF cats (2FB, 4GA) developed no IFNγ mRNA response to all three RBDs, while developing a robust IFNγ mRNA level to ConA stimulation.

Discussion

Our novel finding of cross-reactive Abs to SCoV2 RBD developing in cats during active FCoV infection was unexpected (Fig 1C,1D and 1E) based on low aa sequence similarity at RBD of SCoV2 and FCoVs (Fig 2A and 2C). Hence, the original observation using conventional SCoV2 RBD ELISA was further analyzed and confirmed by more stringent SCoV2 RBD ELISA, immunoblot analysis, *in vitro* FCoV2 infection blocking assay with SCoV2 RBD, and, finally, cellular IFNγ immune responses to SCoV2 RBD. The peak sera from UGAQ2 and all three toms cross-reacted strongly with sensitive SCoV2 RBD ELISA and immunoblot but not with FCoV2 RBD (Fig 3A and 3B). Perhaps the most striking observation was the sera from the toms cross-reacting to SCoV2 RBD with nil-to-minimal reactivity to FCoV2 S glycoprotein on the FCoV2-WV immunoblot (Fig 3C). These results indicate that cross-reactive Abs to SCoV2 RBD appeared without major development of cross-reactive Abs to FCoV2 S glycoprotein, but such results may be different if FCoV1 immunoblot was available for our use. None of our cats (queens, toms, their kittens) developed major NAbs to FCoV2 based on FCoV2 79-1146 NAb assay (Fig 1B). This result further supports our theory that our cats were infected with FCoV1, which was later confirmed by their sera reacting strongly with FCoV1 RBD immunoblot strips (Fig 3D). In addition, the FCoV1 RBD immunoblot strips only reacted with plasma from FCoV1 KU-2 experimentally infected cats but not with plasma from FCoV2 79-1146 inoculated cats (Fig 4E). Conversely, FCoV2 RBD strips only reacted with sera from FCoV2-infected cats but not with plasma from FCoV1-infected cats (Fig 4F).

Unexpectedly, the plasma from FCoV1 KU-2 infected cats did not cross-react to SCoV2 RBD, which was not due to the use of plasma, since all plasma from FCoV2 79-1146 inoculated cats strongly cross-reacted with SCoV2 RBD (Fig 4G). This observation suggests that not all FCoV1-infected cats develop cross-reactive Abs to SCoV2 RBD or

the timing of the plasma collection was possibly too late (60 days post-inoculation). These factors, combined with a) low virus inoculation dose (1-mL/cat of 1 $TCID_{50}$), b) oral/nasal inoculation route, and/or c) low S1/RBD immunogenicity of the infection may have contributed to the lack of SCoV2 RBD cross-reactivity, similar to the lack/loss of cross-reactivity of UGAQ1 and UGAQ3 sera to SCoV2 RBD (Fig 3A).

The fact that our immunoblots are developed under reducing conditions supports our contention that the cross-reacting epitopes on SCoV2 RBD are either linear aa epitopes and/or glycosylated epitope(s). There are a sufficient number of sectional aa sequences similar between SCoV2 and FCoVs (Fig 2 and S3 and S4 Figs) including the additional 12 aa sequence at the carboxyl-end of SCoV2 MB-RBD. Our preliminary FCoV1 RBD immunoblot results with penta-His MAb (Fig 3G) combined with the studies using sera from FCoV1 transmitted or inoculated cats (Figs 3D and 4E) demonstrate that Abs to the glycosylation component of the RBD are present in their sera. This possibility is important since NAbs to glycosylated epitopes have been identified for highly glycosylated HIV-1 envelope and SCoV2 spike glycoprotein [48,49].

Our SPF toms were highly inbred to recognize protective T-cell peptides of both HIV-1 and FIV NC and RT, which contained many HLA-A2 and HLA-B27 peptides (50,51). Hence, there was a remote possibility that our toms' feline leukocyte antigen (FLA) genetics may have contributed to the unexpected cross-reacting Abs to SCoV2 RBD in all of our inbred toms. Consequently, we tested eight laboratory cats living in group housing unrelated to our toms. All tested positive for FCoV infection first by FCoV2-WV ELISA and later confirmed by FCoV2-WV immunoblot analysis (S5A and S5B Fig). The majority of these cats had cross-reacting Abs to SCoV2 RBD, ranging from low to high titers (S5B1 Fig), which were maintained 15 months later. Although these cats were unrelated to our inbred cats, SCoV2 RBD cross-reacting Abs developed in laboratory cats

purchased from the same commercial cat vendor as the UGA queens, but of different cat lineages. This supports the view that the laboratory cats sold by this commercial vendor have lineage(s) with FLA genetic makeup, which may sustain higher titers of cross-reactive Abs to SCoV2 RBD, like cats UGAQ2 and G-2 (Fig 3A and S5B1 Fig). Group-housing appears to sustain the FCoV infection by reinfection without clinical episode. Our preliminary results indicate that FCoV1-infected pet cats in the field possess cross-reactive Abs to SCoV2 RBD without manifesting clinical signs. These observations may also explain why only some SCoV2-infected pet cats display clinical signs while others remain asymptomatic. Such variation in clinical signs was also observed during SCoV2 infection of humans [52,53].

The lack of serum cross-reactivity with FCoV2 S glycoproteins by two of three toms was unexpected since all four queens, including UGAQ2, reacted with FCoV2 S glycoprotein (Fig 3C). This is based on a rationale derived from the fact that both rabbit polyclonal Abs to S2 protein and to S protein cross-reacted with S, degraded S, and S2 of the FCoV2-WV (Fig 3E). Since S2 glycoprotein has high aa sequence identity and similarity, the likelihood of the cross-reactivity with S2 rather than S1 component of the S glycoprotein is a strong possibility based on the study by Zhao *et al.* 2019 [18]. Zhao *et al.* did not observe any serum from 137 FCoV-infected laboratory cats cross-reacting with SCoV1 S1 or other Betacoronaviruses S1 glycoproteins by ELISA. Their report shows serum from 15 FCoV infected cats (10.9%) cross-reacting with HCCoV 229E S1, and the sera from two cats (1.5%) cross-reacting with HCCoV NL63 S1. Both HCCoV 229E and NL63 are human Alphacoronaviruses, and, as stated before, HCCoV 229E uses hAPN as primary cell receptor [27,28], whereas HCCoV NL63 uses hACE2 as primary cell receptor like SCoV1 and SCoV2 [24,54]. None of the 137 sera from FCoV-infected cats cross-reacted with S1 of human SCoV1, MERS-CoV, HCCoV OC43, and HCCoV HKU1

[18]. HCCoV OC43 and HKU1 uses 9-O-acetyylated sialic acid and MERS-CoV2 uses dipeptidylpeptidase 4 (DPP4) as primary cell receptor [55,56]. This study, published in 2019, did not evaluate using the FCoV-WV immunoblot analysis or the cross-reactivity to SCoV2 RBD [18]. SCoV1 RBD has been reported to have 73% aa sequence identity to SCoV2 [34]. Our SCoV1 and SCoV2 S sequence analysis also confirmed their finding of 73% identity and further determined the aa sequence similarity of 90% at RBD and 91.9% at S glycoprotein (S6A and S6B Fig). Our findings show SCoV1 and SCoV2 RBDs have 64.8% identity and 87.9% similarity (S6B Fig). Therefore, our finding that FCoV-infected cats develop cross-reacting Abs to SCoV2 RBD was greatly unexpected when their study showed no cross-reactivity to SCoV1 S1 glycoprotein.

The use of SCoV2 RBD to block the *in vitro* infection of SCoV2 has already been performed and demonstrated by others, blocking the SCoV2 infection of Vero CCL-81 cells with SCoV2 RBD-His tag at IC_{50} of 21 μg/mL [57]. The novelty of our study is that SCoV2 UF-RBD at a high concentration was able to cross-block or cross-protect against FCoV2 infection of feline cell line at a RBD dose of 48-68 μg/mL without any cellular toxicity (Fig 4A). This is slightly more than twice the dose used by Shin *et al.* to block SCoV2 infection of Vero cells with SCoV2 RBD-His [57]. The ability for SCoV2 RBD to cross-protect against in vitro FCoV2 infection, although weaker than that of FCoV2 RBD, further supports our finding that SCoV2 RBD and FCoV2 RBD may be structurally and antigenically similar. We were unable to perform similar blocking study against FCoV1 infection with SCoV2 and FCoV1 RBDs due to the lack of FCoV1-susceptible cell line available [6,29]. Instead the PBMC from transiently and chronically FCoV1-infected cats were used to evaluate whether SCoV2 and FCoV1 RBDs are recognized by the T cells in the PBMC from FCoV1-infected cats. Remarkably the PBMC of both infected cats recognized SCoV2 RBD by producing IFNγ mRNA in response to its stimulation.

However, the FCoV1 RBD stimulation was recognized only by the chronically infected cat. Although a larger number of animals is needed to confirm the results, this observation may suggest that the epitopes in the SCoV2 RBD are similar to those of FCoV1 RBD, while others are possibly more inflammatory than those of FCoV1 RBD. Since IFNγ are mainly produced by $CD4^+$ and $CD8^+$ T cells in the PBMC preparation [58], our observation suggest that the T cells are recognizing these RBDs as having similar T-cell epitopes.

Another interesting observation is that Shin *et al.* used SCoV2 Wuhan RBD, identical to MB-RBD, with the extra 12 aa that had higher aa sequence similarity of SCoV2 RBD, with both FCoV1 and FCoV2 RBDs. Shin *et al.* determined that RBD-Fc tag was better at *in vitro* inhibition of SCoV2 infection than RBD-His [57]. Since FCoV2 RBD had extended amino-end and blocked infection more efficiently, we reasoned that a slightly larger SCoV2 RBD may block the *in vitro* infection against SCoV2 and FCoV2 better than a CoV-nonspecific tag as long as it retains the native conformation. Such RBD in theory must increase anti-SCoV2 cytotoxic T lymphocyte (CTL) epitopes without increasing T-helper epitopes for inflammatory responses. Remarkably our preliminary result shows SCoV2 UF2-RBD (gp40) with strong reactivity to sera from COVID-19 vaccinated humans may achieve these conditions (S7 Fig and S1 Table). Pfizer SCoV2 RBD mRNA vaccine was not as effective as their S mRNA vaccine perhaps due to the shorter RBD sequence and the T4 foldon used [59,60].

The ability of FCoV2 and SCoV2 RBDs to block *in vitro* FCoV2 infection and also induce pan-CoV-specific T-cell responses suggest that these RBDs may be important for developing an effective pan-coronavirus vaccine for pet animals such as cats, dogs, and hamsters. SCoV2 infected hamsters from Europe imported to pet shops in Hong Kong have been reported as a source of two separate hamster-to-human transmissions and subsequent human-to-human transmission of SCoV2 Delta variant, with the sequence

found predominantly in Europe [11]. Inoculation of laboratory Syrian golden hamsters resulted in infection of the hamsters with a major loss in weight, lung infection, and respiratory disease [61,62]. Although not SCoV2, Lednicky *et al.* reported porcine delta-coronavirus infection in three children in Haiti with clinical symptoms of fever and two children also with coughing and abdominal pain [63]. Lednicky *et al.* also discovered a US citizen visiting Haiti who developed fever and malaise [64]. This individual was diagnosed with a coronavirus infection resembling a recombinant of predominantly CCoV with sequences similar to CCoV-HuPn-2018. The CCoV-HuPn-2018 appears to be a recombinant of FCoV2 and CCoV isolated from a patient with pneumonia in East Malaysia [7]. Based on these findings, pan-CoV vaccine that prevents active FCoV and CCoV infections of cats and dogs will indirectly prevent infection of humans, which is another vital role of such a vaccine.

Besides the profound acute severe respiratory syndrome, SCoV2 infection in humans causes gastrointestinal (GI) manifestations (diarrhea, vomiting, nausea, abdominal pain), including longer fecal shedding than those detected in the nasopharyngeal samples [9,65,66]. Both FCoV and CCoV also cause GI tract disease in their respective animal hosts and clinically affect kittens and puppies more than adults, with the exception of FIPV disease [6,23,67]. FCoV2 RBD sequence alignment comparison of CCoV serotype 2 (CCoV2) and FCoV2 RBDs shows 95.6% aa sequence similarity and 87.7% aa sequence identity (S8 Fig). The high sequence similarity between FCoV2 and CCoV2 RBDs may explain why CCoV2 can infect fAPN expressing feline cells [27]. Although FCoV1 and CCoV1 RBDs possess only aa sequence identity of 55.5%, their sequence similarity of 80.8% is remarkably high (S9 Fig), suggesting that they have a common lineage with evolutionary changes and perhaps also by sectional recombination [9,29,67].

Since FCoV infection remained in domestic cats for over three decades [4,5], the FCoV RBDs must have endured the evolutionary pressure and are unlikely to undergo further mutations at RBD to retain its infectivity. Based on these findings, we propose that pan-CoV vaccine against SCoV2 infection in cats, dogs, and hamsters can be developed by combining FCoV1 RBD (gp52) and FCoV2 RBD (gp59) together with a larger SCoV2 RBD (gp40) for stability, potentially without addition of CCoV1/CCoV2 RBDs. However, the addition of conserved pan-CoV CTL epitopes from highly conserved SCoV2/FCoV protein(s) (e.g., RNA-dependent RNA polymerase with minimal mutations among SCoV2 variants) to the triple-RBDs may be required to induce sterilizing immunity (i.e., immunity against infection) in the vaccinated animals. Such pan-CoV vaccine tested in laboratory cats may provide insights on how to develop sterilizing immunity against SCoV2 in humans, while also preventing future zoonotic variant infections and benefiting companion animals.

Methods

Animal populations

The studies used laboratory cats that were bred and cared for under the UF IACUC protocols 200801838 through 202001838, and the sera from pet cats collected under IACUC protocol 201803990. The plasma from Japanese laboratory cats inoculated orally/nasally with either FCoV1 UK-1 or FCoV2 79-1146 (0.8-mL oral and 0.2-mL nasal; 1-mL/cat of 10^5 $TCID_{50}$) and collected at 60 days post-inoculation were kindly provided by Drs. T. Takano and T. Hohdatsu. The SPF toms were inbred from SPF cats initially derived from intact females (Harlan Sprague Dawley, Inc., Indianapolis, IN) and male SPF cats (Cedar River Laboratories, Mason City, IA). Dr. Andrew R. Moorhead of UGA donated four queens (UGAQ1, UGAQ2, UGAQ3, UGAQ4) in fall 2019, which were

initially purchased by UGA from Liberty Research Inc (Waverly, NY). Juvenile cats were generated by mating of the donated queens with the three SPF toms at a UF laboratory. The eight group-housed laboratory cats were initially purchased from Liberty Research, Inc. Their animal code did not show the same lineages as the UGA queens and were considered different cat lineages, unrelated to both UGA queens and UF toms. The second blood collection was obtained 15 months later exception for cat G-5, which was euthanized shortly after the first blood collection for unrelated medical reasons. All cats purchased from Liberty Research, Inc. were vaccinated against rabies using the RABVAC3 vaccine, and feline panleukopenia, calici, and rhinotracheitis viruses, along with hemorrhagic feline calicivirus strain, using the Fel-O-Vax PCT + Calicivax vaccine. Our animal workers, including the Animal Care Service workers, were confirmed negative by RT-PCR for SCoV2 and COVID-19 when working with our cats.

SARS-CoV-2 RBD peptides

Two different versions of SCoV2 were used: the University of Florida-RBD (UF-RBD) and MassBiologics-RBD (MB-RBD). The UF-RBD was produced using Harvard Wuhan RBD plasmid kindly provided by Dr. Aaron G. Schmidt (Ragon Institute) and expressed in EXPI293F cells. UF-RBD had HRV cleavage site, 8x His tag, and streptavidin-binding peptide tag to assist in the purification of the RBD [68]. The MB-RBD was kindly provided by MassBiologics (Boston, MA) under UF/MB MTA and constructed from pcDNA with c-Myc (EQKLISEEDL) and 6x His tags [69].

Feline cell lines

Crandell feline kidney (CrFK) fibroblast, *Felis catus* 9 (Fc9), and *Felis catus* whole fetus-4 (Fcwf-4) cells were provided by Dr. Niels Pederson of the University of California, Davis.

All of these feline cell lines were maintained on Eagle MEM media (Cat. #10-009-CV, Mediatech Inc, Manessas, VA) supplemented with 10% fetal bovine serum (FBS) and 50 µg/mL gentamycin. These cells were maintained at 37°C with 5% CO_2 and passaged every 2–3 days.

Production and partial purification of FCoV2 whole-virus

The CrFK cells were infected with FCoV2 79-1146 (ATCC, Manessas, VA) to produce the stock of crude FCoV2 inoculum for *in vitro* infection studies, and partially purified FCoV2 whole-virus (WV) stock. The infected culture fluids directly from the culture flask (175 cm) were pooled and clarified free of cell debris by low-speed centrifugation at 2800-3000 rpm for 45 min at 5°C. In addition, the freeze-thawed culture fluids from the frozen flasks with residual media were pooled and then clarified free of cell debris by low-speed centrifugation. They were then combined with a portion of the clarified culture fluid from above, from one part clarified direct culture fluid to two parts of clarified cell-debris fluid. The following two methods partially purified both direct and combined clarified fluids. In the first method, the combined clarified fluid was directly concentrated to 10-50 fold by Vivaspin 20 Centrifugal Concentrators (Sartorius, Gottingen, Germany) with PES membrane of 100k MW cut off. The concentrated virus fluid underwent an additional 4-6 washes with PBS using the Centrifugal Concentrator until the phenol red from the culture media was faintly pink in color. This method resulted in a preparation that had a reasonably high FCoV2 load (1.2 mg/mL) with detectable levels of 180 kDa S glycoprotein but almost undetectable BSA (67 kDa). This preparation was used for developing immunoblot strips. The second method consisted of direct concentration of direct-clarified fluid using multiple Centrifugal Concentrators with minimal PBS washes. As a result, this preparation retained the phenol red color and about 5% residual BSA from FBS. This

method provided a virus preparation at a high concentration (150 mg/mL), needed for use in screening a large number of cat sera with FCoV2-WV ELISA.

Transfection and expression of Expi293F Cells with RBD plasmids and purification of RBD proteins

The plasmids pVRC containing human codon-optimized RBD constructs were transiently transfected into Expi293F cells using the ExpiFectamine™ 293 Transfection Kit (Thermo Fisher, Waltham, MA). Briefly, the cell density was adjusted to $3x10^6$ cells/mL in a final volume of 100 mL of Expi293 expression media and allowed to grow 24 h to reach a final density of $5.5x10^6$ cells/mL. The plasmid DNA (1µg/mL) and ExpiFectamine™ 293 reagent were individually diluted with Opti-MEM Reduced Serum Medium (Thermo Fisher, Waltham, MA), incubated 5 min at room temperature (RT), and then mixed together. The ExpiFectamine 293/plasmid DNA mixture was incubated at RT for 20 min and mixed with Expi293F cells. The cells were incubated on an orbital shaker in a 37°C incubator with 8% CO_2. After 24 h of incubation, transfection enhancers-1 and 2 were added and incubated for three days. Then, the cell culture was centrifuged at 1800 x g for 30 min to collect the supernatant for protein purification. The culture supernatant was concentrated to a final volume of 5 mL using a Macrosep Omega Advance Centrifugal Device with a cutoff of 10 kDa (PALL Laboratory, Port Washington, NY). The concentrated supernatant was passed through an equilibrated TALON Metal Affinity Resin (Takara Bio Inc, Shiga, Japan). The column was washed with 10 volume of PBS containing NaCl (300 mM) and imidazole (20 mM) to remove all contaminants. Subsequently, the protein was eluted from the column using PBS containing 250 mM imidazole. The eluted fractions were concentrated using a Nanosep Advance Centrifugal Device with 10K Omega (PALL Laboratory). Estimation of protein purity and quantity were

achieved with SDS-PAGE and a Pierce BCA Protein Assay Kit (Thermo Fisher Scientific, Rockford, IL), respectively.

FCoV-WV and SCoV2 RBD ELISAs with overnight serum incubation

Corning ELISA plate wells were coated with 100µL of 100 µg/mL FCoV2 whole virus antigen or 100 µg/mL SCoV2 RBD or FCoV RBD antigen in sodium bicarbonate ELISA coating buffer at pH 9.5 (BioLegend, San Diego, CA) and incubated overnight at RT. The next day, the plates were washed three times with phosphate-buffered saline tween (PBST). Non-specific binding sites were blocked with 100 µL per well of blocking solution (5% non-fat dry milk in sterile PBST- 0.5% Tween-20) for 1 h at 37°C. After washing with PBST three times, 10 µL of cat serum was diluted in 0.990 mL of blocking solution (1:100) and incubated at RT overnight. After washing, horseradish peroxidase (HRP)-conjugated goat anti-cat IgG diluted 1:4,000 (SouthernBioTech, Birmingham, AL) in PBST was added and incubated at RT for 2 h. After washing, 100 µL of 3,3,5,5-tetramethylbenzidine High Sensitivity Substrate Solution (BioLegend) was added to the wells and incubated at RT for 15 min. The reaction was stopped by adding 100 µL of 1 N HCL in sterile water. The ELISA titer was measured at OD450 using BioTek's Synergy HTX Multi-Mode Microplate Reader (BioTeK, Winooski, VT).

Stringent FCoV-WV and SCoV2 RBD ELISAs

To ensure that the serum ELISA reactivity was specific to the FCoV2-WV, FCoV-RBD, or SCoV2-RBD antigen, sera were incubated individually at the same dilution for only 1 h, instead of overnight. PBS was used instead of bicarbonate buffer for the coating of the antigen on the ELISA plates. Additionally, a BSA antigen control was included since veterinary vaccines used at the time in UGA queens often contained contaminating BSA

from the cell cultures used during the manufacture of viral vaccines. This control was also important because the FCoV2-WV preparation contained about 5% BSA.

Gel and Immunoblot analyses

The purified proteins were analyzed by SDS-PAGE and immunoblot. Briefly, the FCoV2-WV or RBD proteins (100 µg) were boiled individually at 95°C for 5 min in a sample buffer. The protein(s) and prestained marker were loaded into individual wells, separated by 10% Tris-HCL gel with 30% or 40% acrylamide/bis, and stained with Coomassie Blue solution for direct MW analysis or transferred to nitrocellulose membrane. Subsequently, the membrane was treated with Penta-His MAb (Qiagen, Germantown, MD) followed by HRP-conjugated goat anti-mouse IgG (Invitrogen) and HRP substrate for degraded RBD protein/peptide distribution. In the serum reactivity studies, the FCoV2-WV or RBD proteins were evenly loaded into a 7-cm wide well of the stacking gel, with one 4-mm wide well at the end for the prestained marker, separated by 10% Tris-HCL gel with 30% or 40% acrylamide/bis, and transferred to nitrocellulose membrane. Each nitrocellulose blot was cut vertically into 26 3.2-mm width strips using a Novex Model NZ-1CIS strip cutter (Novel Experimental Technology, San Diego, CA). Each immunoblot strip was incubated individually with FCoV-infected cat serum or plasma at a dilution of 1:50 or 1:100 in a blocking buffer and incubated overnight at RT on a rocker. After three washes, the strips were then incubated with alkaline phosphatase (AP)-conjugated goat anti-cat IgG (1:1,000) (SouthernBiotech) for 2 h at RT. Subsequently after three washes, the reactive bands were visualized with freshly mixed AP substrate from AP-Conjugate Substrate Kit (Bio-Rad).

FCoV2 NAb assay against FCoV2

The Fc9 cells were used for both FCoV2 NAb studies and FCoV2/SCoV2 RBD blocking studies against live FCoV2 infection. The FCoV2 NAb assay was a modification of FCoV2 NAb assay as described previously (41). Briefly, the diluted FCoV2 preparation (EMEM culture media with 5% heat-inactivated FBS) at 2 $TCID_{50}$ were plated in a 96-well round-bottom microculture plate and then incubated with an equal volume of serially three-fold diluted cat serum. The plates were incubated at 37°C in a 5% CO_2 incubator for 45 min. The first row of the 12 wells was not used to prevent the drying effect. Thus, the second rows were the most concentrated serum dilutions of 1:6 with the virus preparation. The remaining serum dilutions in the wells were as follows: third rows with 1:18, fourth rows with 1:54, fifth rows with 1:162, sixth rows with 1:486, seventh rows with 1:1458, and eighth rows with 1:4374. Subsequently, 0.1 mL of the mixture of each well was transferred to the flat-bottom wells of Fc9 cell monolayer with 95-97% confluency and incubated for 24 h at 37°C and 5% CO_2. The spent culture fluids were discarded. Each well was aliquoted with 0.1 mL of 0.25% sterile methyl cellulose in EMEM with 5% heat-inactivated FBS, and incubated as before for 18 h or until the 35-50 virus plaques per well were observed. The FCoV2 plaques in the wells were inactivated and stained with 0.1 mL/well of 1% crystal violet in 100% methanol at RT for 10 min. Each well received an additional 0.15 mL of 1% crystal violet in 20% methanol, incubated at RT for 24 h, decanted, and removed the stain with water.

RBD blocking assay against FCoV2

The RBD blocking assay against FCoV2 is a modification of the above FCoV2 NAb assay and differs from the NAb assay by the following three features: 1) A set amount of RBD is used instead of cat serum. 2) FCoV2 dose was 4 $TCID_{50}$ instead of 2 $TCID_{50}$ to assure 95-100% cytopathic effect (CPE) on the Fc9 cells. 3) The flat-bottom plates with Fc9 cells

at 98-100% confluency instead of 95-97% confluency were used when adding the virus mixture. The remaining procedure is identical to the NAb assay.

RBD stimulation of PBMC from FCoV1-infected cats

The PBMC of transiently (4GC) and chronically (G-3) FCoV1-infected cats and two SPF cats (2FB, 4GA) were stimulated with 5 µg/mL of either FCoV1, FCoV2, or SCoV2 RBD in 0.1 mL RPMI 1640 media (Cat. #10040CM, Corning Inc., NY) supplemented with 10% heat-inactivated FBS and 50 µg/mL gentamycin per well in a round-bottom 96-well plate (Costar Cat. #3799, Corning Inc., NY). The plate was incubated for 24 h at 37°C and 5% CO_2, and upon centrifugation, the spent culture fluids were discarded. The cell pellets were washed with PBS before total RNA was extracted with the Direct-zol RNA Micro-Prep method (Cat. R2063-A, Zymo Research Corp., CA), and the extracted RNA was reverse transcribed using LunaScript® RT SuperMix Kit (Cat. NEB #E3010; New England Biolabs, MA). The feline IFNγ mRNA were evaluated using primers (5`AATACCAGCTCCAGTAAACGG 3', & 5`GCTTCCTCAGGTTAGATCTTGG 3`) and FAM-labeled probe (5` FAM-CAGGTCCAGCGCAAAGCAATAAATGA-BHQ 3') in MIC qPCR machine (Bio Molecular Systems, Coomera QLD, Australia). The feline glyceraldehyde-3-phosphate dehydrogenase (*GAPDH*) was used as the housekeeping gene expression using primers (5` ATGTTCCAGTATGATTCCACCC 3`, & 5` ACCAGCATCACCCCATTTG 3`) and FAM-labeled probe (5` FAM-AAATTCCACGGCACAGTCAAGGC-BHQ 3`).

Data Availability: RBD sequences of FCoV1 RBD, FCoV2 RBD, CCoV1 RBD, CCoV2 RBD, SCoV2 UF2-RBD, human codon-optimized FCoV1 RBD, human codon-optimized FCoV2 RBD and human codon-optimized SCoV2 UF2-RBD have been deposited in the NCBI database with accession numbers OP597272, OP597273, OP597274, OP597275, OP597276, OP597277, OP597278 and OP597279, respectively.

Funding: This work was funded by JKY Miscellaneous Donors Account and SK CVM Startup fund 211.

Acknowledgments

We thank Dr, Biao He for providing serum from cat UGA1.4; Dr. Roy Curtiss Jr. for his critical scientific review; Ms. Karen F. Keisling, Lyndsay M. Powers, and Megan R. Di-Lernia for their animal and laboratory assistance; Mr. Charles A. Yowell for pDNA amplification; Ms. Mary E. Bohannon for IACUC assistance; and Ms. Maura C. Pedersen for her editorial assistance. We also thank Dr. Jonathan C. Lee and the pre-veterinary undergraduate students Benjamin Morales, Gwen V. Rohe, Nina M. Beam, Marco B. Prevedello, and Abbey-Gaile Mannings for assisting in animal procedures and the care of the animals.

Author Contributions

Conceptualization: Janet K. Yamamoto, John G. Morris, Jr.

Data curation: Janet K. Yamamoto, Lekshmi K. Edison, Bikash Sahay.

Formal analysis: Janet K. Yamamoto, Lekshmi K. Edison, Bikash Sahay.

Funding acquisition: Janet K. Yamamoto, Subhashinie Kariyawasam.

Investigation: Janet K. Yamamoto, Lekshmi K. Edison, Bikash Sahay, Ananta P. Arukha, Dawne K. Rowe-Haas, Sayaka Shiomitsu, Chiquitha D. Crews, Heather D.S. Walden.

Methodology: Janet K. Yamamoto, Lekshmi K. Edison, Bikash Sahay.

Project Administration: Janet K. Yamamoto, Subhashinie Kariyawasam.

Resources: Dawne K. Rowe-Haas, Stephan M. Tompkins, Tomomi Takano, Tsutomu Hohdatsu, Apichai Tuanyok, Chen Gilor, John G. Morris, Jr.

Supervision: Janet K. Yamamoto, Subhashinie Kariyawasam, Bikash Sahay.

Visualization: Janet K. Yamamoto, Lekshmi K. Edison, Bikash Sahay.

Writing – original draft: Janet K. Yamamoto, Lekshmi K. Edison, Subhashinie Kariyawasam.

Writing – review & editing: Janet K. Yamamoto, Lekshmi K. Edison, Bikash Sahay, Tomomi Takano, Tsutomu Hohdatsu, Apichai Tuanyok, Chen Gilor.

References:

1. Zhou Q, Li Y, Huang J, Fu N, Song X, Sha X, et al. Prevalence and molecular characteristics of feline coronavirus in southwest China from 2017 to 2020. J Gen Virol. 2021;102. http://doi:10.1099/jgv.0.001654 PMID: 34524074
2. Klein-Richers U, Hartmann K, Hofmann-Lehmann R, Unterer S, Bergmann M, Rieger A, et al. Prevalence of feline coronavirus shedding in German catteries and associated risk factors. Viruses. 2020;12: 1000. http://doi:10.3390/v12091000 PMID: 32911718; PubMed Central PMCID: PMC7551668
3. McKay LA, Meachem M, Snead E, Brannen T, Mutlow N, Ruelle L, et al. Prevalence and mutation analysis of the spike protein in feline enteric coronavirus and feline infectious peritonitis detected in household and shelter cats in western Canada. Can J Vet Res. 2020;84: 18-23. PMID: 31949325; PubMed Central PMCID: PMC6921991
4. Horzinek MC, Osterhaus AD. The virology and pathogenesis of feline infectious peritonitis. Brief review. Arch Virol. 1979;59: 1-15. http://doi:10.1007/BF01317889 PMID: 218528; PubMed Central PMCID: PMC7087126
5. Vennema H, Poland A, Foley J, Pedersen NC. Feline infectious peritonitis viruses arise by mutation from endemic feline enteric coronaviruses. Virology. 1998;243: 150-157. http://doi:10.1006/viro.1998.9045 PMID: 9527924, PubMed Central PMCID: PMC7131759
6. Pedersen NC. An update on feline infectious peritonitis: virology and immunopathogenesis. Vet J. 2014;201: 123-132. http://doi:10.1016/j.tvjl.2014.04.017 PMID: 24837550; PubMed Central PMCID: PMC7110662
7. Vlasova AN, Diaz A, Damtie D, Xiu L, Toh TH, Lee JS, et al. Novel canine coronavirus isolated from a hospitalized patient with pneumonia in East Malaysia. Clin Infect Dis. 2022;74: 446-454. http://doi:10.1093/cid/ciab456 PMID: 34013321; PubMed Central PMCID: PMC8194511
8. Silva CS, Mullis LB, Pereira O, Saif LJ, Vlasova A, Zhang X, et al. Human respiratory coronaviruses detected in patients with influenza-like illness in Arkansas, USA. Virol Mycol. 2014;2014. http://doi:10.4172/2161-0517.S2-004 PMID: 27588218; PubMed Central PMCID: PMC5004774
9. Vlasova AN, Toh TH, Lee JS, Poovorawan Y, Davis P, Azevedo MSP, et al. Animal alphacoronaviruses found in human patients with acute respiratory illness in different countries. Emerg Microbes Infect. 2022;11: 699-702. http://doi:10.1080/22221751.2022.2040341 PMID: 35156544; PubMed Central PMCID: PMC8890521
10. Pagani G, Lai A, Bergna A, Rizzo A, Stranieri A, Giordano A, et al. Human-to-cat SARS-CoV-2 transmission: case report and full-genome sequencing from an infected pet and its owner in northern Italy. Pathogens. 2021;10: 252. http://doi:10.3390/pathogens10020252 PMID: 33672421; PubMed Central PMCID: PMC7926546
11. World Organization for Animal Health, Global cases of SARS-CoV-2 in animals. (Note this website provides information about each animal case with some clinical history). Available from: https://www.oie.int/en/what-we-offer/emergency-and-resilience/covid-19/#ui-id-3 (Report ID FUR_154029 describes hamster-to-human transmission of SCoV2 Delta variant.).

12. USDA. Confirmed cases of SARS-CoV-2. last Updated 23 March, 2022 https://www.aphis.usda.gov/aphis/ourfocus/onehealth/one-health-sarscov2-in-animals. In: Animals in the United States.
13. Shi J, Wen Z, Zhong G, Yang H, Wang C, Huang B, et al. Susceptibility of ferrets, cats, dogs, and other domesticated animals to SARS-coronavirus 2. Science. 2020;368: 1016-1020. http://doi:10.1126/science.abb7015 PMID: 32269068; PubMed Central PMCID: PMC7164390
14. Bosco-Lauth AM, Hartwig AE, Porter SM, Gordy PW, Nehring M, Byas AD, et al. Experimental infection of domestic dogs and cats with SARS-CoV-2: pathogenesis, transmission, and response to reexposure in cats. Proc Natl Acad Sci U S A. 2020;117: 26382-26388. http://doi:10.1073/pnas.2013102117 PMID: 32994343; PubMed Central PMCID: PMC7585007
15. Gaudreault NN, Trujillo JD, Carossino M, Meekins DA, Morozov I, Madden DW, et al. SARS-CoV-2 infection, disease and transmission in domestic cats. Emerg Microbes Infect. 2020;9: 2322-2332. http://doi:10.1080/22221751.2020.1833687 PMID: 33028154; PubMed Central PMCID: PMC7594869
16. Sit THC, Brackman CJ, Ip SM, Tam KWS, Law PYT, To EMW, et al. Infection of dogs with SARS-CoV-2. Nature. 2020;586: 776-778. http://doi:10.1038/s41586-020-2334-5 PMID: 32408337; PubMed Central PMCID: PMC7606701
17. Vlasova AN, Zhang X, Hasoksuz M, Nagesha HS, Haynes LM, Fang Y, et al. Two-way antigenic cross-reactivity between severe acute respiratory syndrome coronavirus (SARS-CoV) and Group 1 animal CoVs is mediated through an antigenic site in the N-terminal region of the SARS-CoV nucleoprotein. J Virol. 2007;81: 13365-13377. http://doi:10.1128/JVI.01169-07 PMID: 17913799; PugMed Central PMCID: PMC2168854
18. Zhao S, Li W, Schuurman N, van Kuppeveld F, Bosch B-J, Egberink H. Serological screening for conronavirus infections in cats. Viruses. 2019;11: 743. http://doi:10.3390/v11080743 PMID: 31412572; PubMed Central PMCID: PMC6723642
19. Wrapp D, Wang N, Corbett KS, Goldsmith JA, Hsieh CL, Abiona O, et al. Cryo-EM structure of the 2019-nCoV spike in the prefusion conformation. Science. 2020;367: 1260-1263. http://doi:10.1126/science.abb2507 PMID: 32075877; PubMed Central PMCID: PMC7164637
20. Skowronski DM, Astell C, Brunham RC, Low DE, Petric M, Roper RL, et al. Severe acute respiratory syndrome (SARS): A year in review. Annu Rev Med. 2005;56: 357-381. http://doi:10.1146/annurev.med.56.091103.134135 PMID: 15660517
21. Guan Y, Zheng BJ, He YQ, Liu XL, Zhuang ZX, Cheung CL, et al. Isolation and characterization of viruses related to the SARS coronavirus from animals in southern China. Science. 2003;302: 276-278. http://doi:10.1126/science. 1087139 PMID: 12958366
22. Martina BEE, Haagmans BL, Kuiken T, Fouchier RA, Rimmelzwaan GF, Van Amerongen G, et al. Virology: SARS virus infection of cats and ferrets. Nature. 2003;425: 915. http://doi:10.1038/425915a PMID: 14586458; PubMed Central PMCID: PMC7094990
23. Stout AE, André NM, Jaimes JA, Millet JK, Whittaker GR. Coronaviruses in cats and other companion animals: where does SARS-CoV-2/COVID-19 fit? Vet Microbiol.

2020;247: 108777. http://doi:10.1016/j.vetmic.2020.108777 PMID: 32768223; PubMed Central PMCID: PMC7309752

24. Tai W, He L, Zhang X, Pu J, Voronin D, Jiang S, et al. Characterization of the receptor-binding domain (RBD) of 2019 novel coronavirus: implication for development of RBD protein as a viral attachment inhibitor and vaccine. Cell Mol Immunol. 2020;17: 613-620. http://doi:10.1038/s41423-020-0400-4 PMID: 32203189; PubMed Central PMCID: PMC7091888
25. Hohdatsu T, Izumiya Y, Yokoyama Y, Kida K, Koyama H. Differences in virus receptor for type I and type II feline infectious peritonitis virus. Arch Virol. 1998;143: 839-850. http://doi:10.1007/s007050050336 PMID: 9645192; PubMed Central PMCID: PMC7087195
26. Dye C, Temperton N, Siddell SG. Type I feline coronavirus spike glycoprotein fails to recognize aminopeptidase N as a functional receptor on feline cell lines. J Gen Virol. 2007;88: 1753-1760. http://doi:10.1099/vir.0.82666-0 PMID: 17485536; PubMed Central PMCID: PMC2584236
27. Tusell SM, Schittone SA, Holmes KV. Mutational analysis of aminopeptidase N, a receptor for several group 1 coronaviruses, identifies key determinants of viral host range. J Virol. 2007;81: 1261-1273. http://doi:10.1128/JVI.01510-06 PMID: 17093189; PubMed Central PMCID: PMC1797531
28. Kolb AF, Hegyi A, Siddell SG. Identification of residues critical for the human coronavirus 229E receptor function of human aminopeptidase N. J Gen Virol. 1997;78: 2795-2802. http://doi:10.1099/0022-1317-78-11-2795 PMID: 9367365
29. Jaimes JA, Millet JK, Stout AE, André NM, Whittaker GR. A tale of two viruses: the distinct spike glycoproteins of feline coronaviruses. Viruses. 2020;12: 83. http://doi10.3390/v12010083 PMID: 31936749; PubMed Central PMCID: PMC7019228
30. An DJ, Jeoung HY, Jeong W, Park JY, Lee MH, Park BK. Prevalence of Korean cats with natural feline coronavirus infections. Virol J. 2011;8: 455. http://doi:10.1186/1743-422X-8-455 PMID: 21951835; PubMed Central PMCID: PMC3219666
31. Terada Y, Matsui N, Noguchi K, Kuwata R, Shimoda H, Soma T, et al. Emergence of pathogenic coronaviruses in cats by homologous recombination between feline and canine coronaviruses. PLOS ONE. 2014;9: e106534. http://doi:10.1371/journal.pone.0106534 PMID: 25180686; PubMed Central PMCID: PMC4152292
32. Wu L, Chen Q, Liu K, Wang J, Han P, Zhang Y, et al. Broad host range of SARS-CoV-2 and the molecular basis for SARS-CoV-2 binding to cat ACE2. Cell Discov. 2020;6: 68. http://doi:10.1038/s41421-020-00210-9 PMID: 33020722; PubMed Central PMCID: PMC7526519
33. Conceicao C, Thakur N, Human S, Kelly JT, Logan L, Bialy D, et al. The SARS-CoV-2 spike protein has a broad tropism for mammalian ACE2 proteins. PLOS Biol. 2020;18: e3001016. http://doi:10.1371/journal.pbio.3001016 PMID: 33347434; PubMed Central PMCID: PMC7751883
34. Wan Y, Shang J, Graham R, Baric RS, Li F. Receptor recognition by the novel coronavirus from Wuhan: an analysis based on decade- long structural studies of SARS coronavirus. J Virol. 2020;94: e00127-20. http://doi:10.1128/JVI.00127-20 PMID: 31996437; PubMed Central PMCID: PMC7081895

35. Chan JF, Kok KH, Zhu Z, Chu H, To KK, Yuan S, et al. Genomic characterization of the 2019 novel human-pathogenic coronavirus isolated from a patient with atypical pneumonia after visiting Wuhan. Emerg Microbes Infect. 2020;9: 221-236. http://doi:10.1080/22221751.2020.1719902 PMID: 31987001; PubMed Central PMCID: PMC7067204
36. Zhou H, Chen X, Hu T, Li J, Song H, Liu Y, et al. A novel bat coronavirus closely related to SARS-CoV-2 contains natural insertions at the S1/S2 cleavage site of the spike protein. Curr Biol. 2020;30: 2196-2203.e3. http://doi:10.1016/j.cub.2020.05.023 PMID: 32416074; PubMed Central PMCID: PMC7211627
37. Regan AD, Millet JK, Tse LP, Chillag Z, Rinaldi VD, Licitra BN, et al. Characterization of a recombinant canine coronavirus with a distinct receptor-binding (S1) domain. Virology. 2012;430: 90-99. http://doi:10.1016/j.virol.2012.04.013 PMID: 22609354; PubMed Central PMCID: PMC3377836
38. Li C, Li W, Lucio de Esesarte E, Guo H, van den Elzen P, Aarts E, et al. Cell attachment domains of the porcine epidemic diarrhea virus spike protein are key targets of neutralizing antibodies. J Virol. 2017;91: e00273-17. http://doi:10.1128/JVI.00273-17 PMID: 28381581; PubMed Central PMCID: PMC5446644
39. Reguera J, Ordoño D, Santiago C, Enjuanes L, Casasnovas JM. Antigenic modules in the N-terminal S1 region of the transmissible gastroenteritis virus spike protein. J Gen Virol. 2011;92: 1117-1126. http://doi:10.1099/vir.0.027607-0 PMID: 21228126; PubMed Central PMCID: PMC3139418
40. Shirato K, Maejima M, Islam MT, Miyazaki A, Kawase M, Matsuyama S, et al. Porcine aminopeptidase N is not a cellular receptor of porcine epidemic diarrhoea virus, but promotes its infectivity via aminopeptidase activity. J Gen Virol. 2016;97: 2528-2539. http://doi:10.1099/jgv.0.000563 PMID: 27449937
41. Kida K, Hohdatsu T, Fujii K, Koyama H. Selection of antigenic variants of the S glycoprotein of feline infectious peritonitis virus and analysis of antigenic sites involved in neutralization. J Vet Med Sci. 1999;61: 935-938. http://doi:10.1292/jvms.61.935 PMID: 10487234
42. Corapi WV, Darteil RJ, Audonnet JC, Chappuis GE. Localization of antigenic sites of the S glycoprotein of feline infectious peritonitis virus involved in neutralization and antibody-dependent enhancement. J Virol. 1995;69: 2858-2862. http://doi:10.1128/JVI.69.5.2858-2862.1995 PMID: 7707508; PubMed Central PMCID: PMC188981
43. AP report. Governor: Florida has first cases of coronavirus. https://www.wesh.com/article/florida-gov-says-coronvirus-2-presumptively-positive-tests/31180562.
44. Coutard B, Valle C, de Lamballerie X, Canard B, Seidah NG, Decroly E. The spike glycoprotein of the new coronavirus 2019-nCoV contains a furin-like cleavage site absent in CoV of the same clade. Antiviral Res. 2020;176: 104742. http://doi:10.1016/j.antiviral.2020.104742 PMID: 32057769; PubMed Central PMCID: PMC7114094
45. Millet JK, Whittaker GR. Host cell proteases: critical determinants of coronavirus tropism and pathogenesis. Virus Res. 2015;202: 120-134. http://doi:10.1016/j.virusres.2014.11.021 PMID: 25445340; PubMed Central PMCID: PMC4465284

46. Pinto D, Park YJ, Beltramello M, Walls AC, Tortorici MA, Bianchi S, et al. Cross-neutralization of SARS-CoV-2 by a human monoclonal SARS-CoV antibody. Nature. 2020;583(7815): 290-295. http://doi:10.1038/s41586-020-2349-y PMID: 32422645
47. S. E. Aillo, M. A. Moses, “Feline infectious peritonitis: Management of multi-cat households” in The Merck Veterinary Manual; Chapter: Generalized Conditions, eleventh eds. (2016), pp. 788.
48. Follis KE, York J, Nunberg JH. Furin cleavage of the SARS coronavirus spike glycoprotein enhances cell-cell fusion but does not affect virion entry. Virology. 2006;350: 358-369. http://doi:10.1016/j.virol.2006.02.003 PMID: 16519916; PubMed Central PMCID: PMC7111780
49. Calarese DA, Lee HK, Huang CY, Best MD, Astronomo RD, Stanfield RL, et al. Dissection of the carbohydrate specificity of the broadly neutralizing anti-HIV-1 antibody 2G12. Proc Natl Acad Sci U S A. 2005;102: 13372-13377. http://doi:10.1073/pnas.0505763102 PMID: 16174734 PubMed Central PMCID: PMC1224641
50. Aranyos AM, Roff SR, Pu R, Owen JL, Coleman JK, Yamamoto JK. An initial examination of the potential role of T-cell immunity in protection against feline immunodeficiency virus (FIV) infection. Vaccine. 2016;34: 1480-1488. http://doi:10.1016/j.vaccine.2016.01.017 PMID: 26802606; PubMed Central PMCID: PMC4775318
51. Sahay B, Aranyos AM, Mishra M, McAvoy AC, Martin MM, Pu R, et al. Immunogenicity and efficacy of a novel multi-antigenic peptide vaccine based on cross-reactivity between feline and human immunodeficiency viruses. Viruses. 2019;11: 136. http://doi:10.3390/v11020136 PMID: 30717485; PubMed Central PMCID: PMC6409633
52. Sakurai A, Sasaki T, Kato S, Hayashi M, Tsuzuki SI, Ishihara T, et al. Natural history of asymptomatic SARS-CoV-2 infection. N Engl J Med. 2020;383: 885-886. http://doi:10.1056/NEJMc2013020 PMID: 32530584; PubMed Central PMCID: PMC7304419
53. Meyerowitz EA, Richterman A, Bogoch II, Low N, Cevik M. Towards an accurate and systematic characterisation of persistently asymptomatic infection with SARS-CoV-2. Lancet Infect Dis. 2021;21: e163-e169. http://doi:10.1016/S1473-3099(20)30837-9 PMID: 33301725; PubMed Central PMCID: PMC7834404
54. Hofmann H, Pyrc K, van der Hoek L, Geier M, Berkhout B, Pöhlmann S. Human coronavirus NL63 employs the severe acute respiratory syndrome coronavirus receptor for cellular entry. Proc Natl Acad Sci U S A. 2005;102: 7988-7993. http://doi:10.1073/pnas.0409465102 PMID: 15897467; PubMed Central PMCID: PMC1142358
55. Hulswit RJG, Lang Y, Bakkers MJG, Li W, Li Z, Schouten A, et al. Human coronaviruses OC43 and HKU1 bind to 9-O-acetylated sialic acids via a conserved receptor-binding site in spike protein domain A. Proc Natl Acad Sci U S A. 2019;116: 2681-2690. http://doi:10.1073/pnas.1809667116 PMID: 30679277; PubMed Central PMCID: PMC6377473
56. Raj VS, Mou H, Smits SL, Dekkers DH, Müller MA, Dijkman R, et al. Dipeptidyl peptidase 4 is a functional receptor for the emerging human coronavirus-EMC. Nature. 2013;495: 251-254. http://doi:10.1038/nature12005 PMID: 23486063; PubMed Central PMCID: PMC7095326

57. Shin HJ, Ku KB, Kim HS, Moon HW, Jeong GU, Hwang I, et al. Receptor-binding domain of SARS-CoV-2 spike protein efficiently inhibits SARS-CoV-2 infection and attachment to mouse lung. Int J Biol Sci. 2021;17: 3786-3794. http://doi:10.7150/ijbs.61320 PMID: 34671199; PubMed Central PMCID: PMC8495392
58. Roff SR, Noon-Song EN, Yamamoto JK. The significance of interferon-γ in HIV-1 pathogenesis, therapy, and prophylaxis. Front Immunol. 2014;4:498/1-11. http://doi:10.3389/fimmu.2013.00498 PMID: 24454311
59. Walsh EE, Frenck RW, Falsey AR, Kitchin N, Absalon J, Gurtman A, et al. Safety and immunogenicity of two RNA-based Covid-19 vaccine candidates. N Engl J Med. 2020;383: 2439-2450. http://doi:10.1056/NEJMoa2027906 PMID: 33053279; PubMed Central PMCID: PMC7583697
60. Vogel AB, Kanevsky I, Che Y, Swanson KA, Muik A, Vormehr M, et al. BNT162b vaccines protect rhesus macaques from SARS-CoV-2. Nature. 2021;592: 283-289. http://doi:10.1038/s41586-021-03275-y PMID: 33524990
61. Sia SF, Yan LM, Chin AWH, Fung K, Choy KT, Wong AYL, et al. Pathogenesis and transmission of SARS-CoV-2 in golden hamsters. Nature. 2020;583: 834-838. http://doi:10.1038/s41586-020-2342-5 PMID: 32408338; PubMed Central PMCID: PMC7394720
62. Abdelnabi R, Boudewijns R, Foo CS, Seldeslachts L, Sanchez-Felipe L, Zhang X, et al. Comparing infectivity and virulence of emerging SARS-CoV-2 variants in Syrian hamsters. EBiomedicine. 2021;68: 103403. http://doi:10.1016/j.ebiom.2021.103403 PMID: 34049240 PMCID: PMC8143995
63. Lednicky JA, Tagliamonte MS, White SK, Elbadry MA, Alam MM, Stephenson CJ, et al. Independent infections of porcine Deltacoronavirus among Haitian children. Nature. 2021;600: 133-137. http://doi:10.1038/s41586-021-04111-z PMID: 34789872; PubMed Central PMCID: PMC8636265
64. Lednicky JA, Tagliamonte MS, White SK, Blohm GM, Alam MM, Iovine NM, et al. Isolation of a novel recombinant canine coronavirus from a visitor to Haiti: further evidence of transmission of coronaviruses of zoonotic origin to humans. Clin Infect Dis. 2022;75: e1184-e1187. http://doi:10.1093/cid/ciab924 PMID: 34718467; PubMed Central PMCID: PMC9402678
65. Díaz LA, García-Salum T, Fuentes-López E, Reyes D, Ortiz J, Chahuan J, et al. High prevalence of SARS-CoV-2 detection and prolonged viral shedding in stools: A systematic review and cohort study. Gastroenterol Hepatol (N Y). 2022;5705: 00001-00002. http://doi:10.1016/j.gastrohep.2021.12.009 PMID: 35077722; PubMed Central PMCID: PMC8783395
66. Galanopoulos M, Karianakis G, Amorginos K, Doukatas A, Gkeros F, Tsoukalas N, et al. Laboratory manifestations and pathophysiological aspects of coronavirus disease 2019 pandemic: focusing on the digestive system. Eur J Gastroenterol Hepatol. 2021;33: e59-e65. http://doi:10.1097/MEG.0000000000002068 PMID: 35048645
67. Licitra BN, Duhamel GE, Whittaker GR. Canine enteric coronaviruses: emerging viral pathogens with distinct recombinant spike proteins. Viruses. 2014;6: 3363-3376. http://doi:10.3390/v6083363 PMID: 25153347; PubMed Central PMCID: PMC4147700
68. Nanishi E, Borriello F, O'Meara TR, McGrath ME, Saito Y, Haupt RE, et al. An aluminium hydroxide: CpG adjuvant enhances protection elicited by a SARS-CoV-2

receptor binding domain vaccine in aged mice. Sci Transl Med. 2022;14: eabj5305. http://doi:10.1126/scitranslmed.abj5305 PMID: 34783582

69. Yates JL, Ehrbar DJ, Hunt DT, Girardin RC, Dupuis AP 2nd, Payne AF, et al. Serological analysis reveals an imbalanced IgG subclass composition associated with COVID-19 disease severity. Cell Rep Med. 2021;2(7):100329. http://doi:10.1016/j.xcrm.2021.100329 PMID: 34151306; PubMed Central PMCID: PMC8205277

Figure Legend

Fig 1. Serum Ab reactivity of the FCoV-positive cats to FCoV2 whole-virus and SCoV2 RBD antigens by ELISA. Four queens (UGAQ1, UGAQ2, UGAQ3, UGAQ4) were mated at UF with three SPF toms (5HQT1, HOJT2, HOGT3). In the first harem breeding cycle (A), only two of the four queens (UGAQ3, UGAQ4) successfully mated with two different toms (5HQT1, HOJT2) gave birth to kittens. Queen UGAQ3 mated with 5HQT1 and gave birth to Y2B (A), and their bars are represented with slashes (B,C). Queen UGAQ4 mated with HOJT2 and gave birth to D4A, D4D, D4F, and D4B (A), and the bars of D4A, D4D, and D4F are represented with small dots (B,C). At the time of first blood collection, these kittens were juvenile cats at 16 weeks old for D4A, D4D, and D4F and 12 weeks old for Y2B (A). The open bars are the two queens UGAQ1 and UGAQ2 (B,C) that were also harem mated with toms 5HQT1 and HOJT2 respectively but did not give birth to kittens in the first mating as well as in the pair mating for UGAQ2 (A). The serum from FCoV2-seropositive cat UGA1.4 (B) and SCoV2 inoculated cat UGA4.1 (C) were used as positive control serum. The serum from SPF cats HOE (B) and BDN (C) were used as negative control serum. The FCoV2 NAb titers shown below the cat identification code (B) were those measured at first arrival for queens and post-first mating for toms. FCoV2 NAb assays were performed thrice for repeatability. The sera from the later timepoints described in Figures 1D and 1E were tested twice and had no detectable NAbs (data not shown). Additionally, the serum Ab cross-reactivity of four $FCoV^+$ queens (D) at post-UF arrival in months (mo) and three toms (E) at pre-mating and post-first mating with the $FCoV^+$ queens was tested by stringent ELISA. Their sera were tested for reactivity to FCoV2-WV (grey bar), SCoV2 UF-RBD (light blue bar), SCoV2 MB-RBD (blue bar), and BSA (white bar). Significant difference between the pre-mating and post mating sera of the respective bars are shown as $p<0.05$ (*) or $p<0.005$ (**) (E). The serum from SPF cat HOE was used as a negative control for all three antigens (D,E). The same sera from the toms tested negative for anti-BSA Ab titers before this set of ELISA assays (S1B Fig).

Fig 2. Amino acid (aa) sequence alignment of SCoV2 Wuhan RBD along with proposed FCoV1 RBD (A) and with proposed FCoV2 RBD (B) using multi-alignment analysis with four FCoV strains. In order to prevent one strain anomaly, four strains of FCoV1 (A) were aligned with SCoV2 Wuhan RBD by Clustal Omega 1.2.1 of JustBio Server (https://justbio.com/). The SCoV2 Wuhan RBD sequence is shown at the top in blue, and the SCoV2 receptor binding motif (RBM) is underlined. Magenta-colored RBD sequence belongs to the proposed FCoV1 UCD-1 RBD sequence (*A*, second FCoV1 sequence) and the proposed FCoV2 79-1146 RBD sequence (B, fourth FCoV2 sequence). The blue-labeled residues below the MB-RBD bracket represent the MassBiologic's SCoV2 RBD with the extra 12 residues. The identical and similar aa residues are shown with an asterisk (*) for complete identity, strong similarity with a colon (:), and modest similarity with a single dot (.). The gaps are shown with a dash (-). The aa sequence identity and similarity for UF-RBD (without carboxyl-end 12 aa residues) and MB-RBD sequences are summarized (C), starting with arginine (R) on the amino-end of SCoV2 pointed downward with a red arrow and ending with an upward red arrow, with the number of aa for UF-RBD or MB-RBD with gaps. Next, the proposed FCoV1 UCD-1 RBD sequence (aa residues 406-684) and the proposed FCoV2 79-1146 RBD sequence (aa residues 408-675) were aligned similarly using JustBio Server (D). The bolded, underlined sections represent potential RBM regions, based on counterpart SCoV2 RBM regions in Figures S2 for FCoV2 79-1146 and S3 for FCoV1 UCD-1. The FCoV1 UCD-1 RBD has three N-glycosylation sites with a high prediction as shown with bolded red **N** and no O-glycosylation, based on the NetNGlyc 1.0 Server and NetOGlyc 4.1 Server, respectively (network address in Figure S1 legend). FCoV2 79-1146 RBD has four predicted N-glycosylation sites (**N**), shown in bold red, and one O-glycosylation site in bold bright-blue (**T**). The aa sequence identity and similarity between the two RBD sequences are summarized (E), starting with asparagine (N) with a start arrow and ending with an end arrow.

The six color coded symbols below the FCoV2 79-1146 sequence represent six nMAbs identified by Kida *et al.* in blue [41] and Corapi *et al.* in red [42], and these nMAbs were produced using FCoV2 79-1146. The three nMAbs of Kida *et al.* do not cross-neutralize FCoV1 virus (T. Hohdatsu, coauthor of this article and reference [41]).

Fig 3. Immunoblot analyses of the sera from FCoV$^+$ queens and SCoV2 RBD-positive toms followed by MW analyses of the RBDs. Immunoblots were developed to the SCoV2 UF-RBD (A), the proposed FCoV2 RBD (B), the cross-reactive FCoV2-WV (C), and the proposed FCoV1 RBD (D). Similar to Figures 1D and 1E, the time of serum collection from four FCoV$^+$ queens are shown as time post arrival to UF, and those from the toms are shown as time post-first exposure to a FCoV$^+$ queen. The MW size range for the RBD bands SCoV2, FCoV2, and FCoV1 are shown next to the control bands. The bands for FCoV2 structural proteins in FCoV2-WV immunoblot (C) are 43 kDa for NC (long arrow), 28-32 kDa for M (long arrow), and 80-90 kDa for spike-2 glycoprotein (S2) (arrow head). The 190 kDa band (short arrow) in the FCoV2-WV immunoblot strips is the S glycoprotein confirmed by a cross-reactivity analysis using rabbit polyclonal antibodies (pAb) to SCoV2 S2 (Sigma ABF1063) and to SCoV2 S (Sigma ABF1066) which cross-reacted with FCoV2 S2 and S, respectively (E1). The rabbit pAb to SCoV2 S1 (Sigma ABF1065) did not cross-react with FCoV2 S1 on immunoblot. Consequently, it served as rabbit control pAb to detect non-specific trapping of the rabbit pAb to the FCoV2 S2 band which had the highest antigen load on the immunoblot. The same analysis was performed at three serum dilutions for UGAQ4 and three toms (HOJT2, HOGT3, 5HQT1), with UGAQ2 only at 1:1000 using the immunoblot of the same batch (E2). All immunoblot photographs were adjusted for consistency to 10% brightness and 5% contrast. The actual MW of the RBDs used in the immunoblot analyses was determined by Coomassie Blue staining of RBD gel (F) and Penta-His MAb treated RBD immunoblot (G). The SCoV2 UF-RBD, FCoV1 RBD, and FCoV2 RBD used the same plasmid with cleavage site peptide and two tags (70 aa with MW of 7,454 Da) attached on the carboxyl-end (S1 Fig). The SCoV2 MB-RBD had c-Myc peptide tag and 6x His Tag (16 aa with MW of 1202 Da) besides the additional 12 aa extension of the RBD (S1 Fig). The predicted MW without attachment (w/o Tag) (F), predicted MW without Tag and glycan (G) and the predicted glycan MW (G) are shown. The blue arrows represent the location of the peptide band within the major glycosylation band (F). The red arrow points to the sharp thin glycosylated band (F), which is an extremely thin peptide line indicated by a red arrow in the immunoblot (G). These results highlighted with the red arrows together with the thin glycosylated band immediately above the major glycosylated peptide band in panel D indicate that FCoV1 infected cats develop antibodies also to the glycosylation component of the RBD.

Fig 4. The *in vitro* FCoV2 infection blocking activity of the proposed FCoV2 RBD and the SCoV2 RBD followed by the immunoblot analyses of the sera from FCoV-inoculated cats. In Plate A (A), the lanes consisted of media control without virus (rows 2-8, lane 1), virus control (rows 2-8, lane 2), SCoV2 RBD starting at 64.2 ug/mL (row 2, lanes 3-4), SCoV2 RBD starting at 42.8 ug/mL (row 2, lanes 5-6), FCoV2 RBD starting at 2.86 ug/mL (row 2, lanes 7-8), 0.075 mL of PBS in first well (row 2, lanes 9-10), and 0.05 mL PBS in first well (row 2, lanes 11-12). Each well in lanes 3-12 starting from row 3 are serial three-fold dilutions of the RBD or PBS. The RBD stocks were suspended in PBS, and the PBS lanes represent the largest volume of the SCoV2 RBD (0.075 mL) and FCoV2 RBD (0.050 mL) used in the wells in row 2. Plate B (B) used the same plating scheme but had duplicate wells of FCoV2 RBD in ten-fold dilution in row 2 as described on the bottom. The 0.05 mL PBS control represents the largest volume of FCoV2 RBD used. The red horizontal double arrow shows where the blocking effect of the RBD stops when directly observed at the plate in plates A and B. The control Plate C (C) are the highest amounts used for SCoV2 RBD and FCoV2 RBD for Plate A tested without virus to determine the potential cell toxicity caused by the RBDs. After scanning the plates at 100% brightness and 70% contrast,

the plates were additionally brightened by 25% for plates A and C and 30% for Plate B with all plates at additional 3% contrast. Next, the plasma from five FCoV1 KU-2-inoculated laboratory cats and six FCoV2 79-1146-inoculated laboratory cats were tested for their immunoblot reactivity to FCoV2-WV (D), FCoV1 RBD (E), FCoV2 RBD (F), and SCoV2 RBD (G). The serum from two SPF cats HOE and HOF served as the negative controls (D-G). Additional positive control serum from SCoV2 inoculated cat UGA4.4 was included for SCoV2 RBD immunoblot (G). All immunoblot photographs were adjusted to 12% brightness and 5% contrast for consistency. (H) Lastly, the PBMC of transiently and chronically FCoV1-infected cats (4GC, G-3) were stimulated with either FCoV1 (red), FCoV2 (blue), or SCoV2 (green) RBD. The expression of IFNγ of each stimulated PBMC is presented as the relative transcription of IFNγ mRNA level relative to the GAPDH mRNA level using qRT-PCR. The stimulation of T-cell mitogen ConA served as a positive control, whereas the RPMI media served as a negative control.

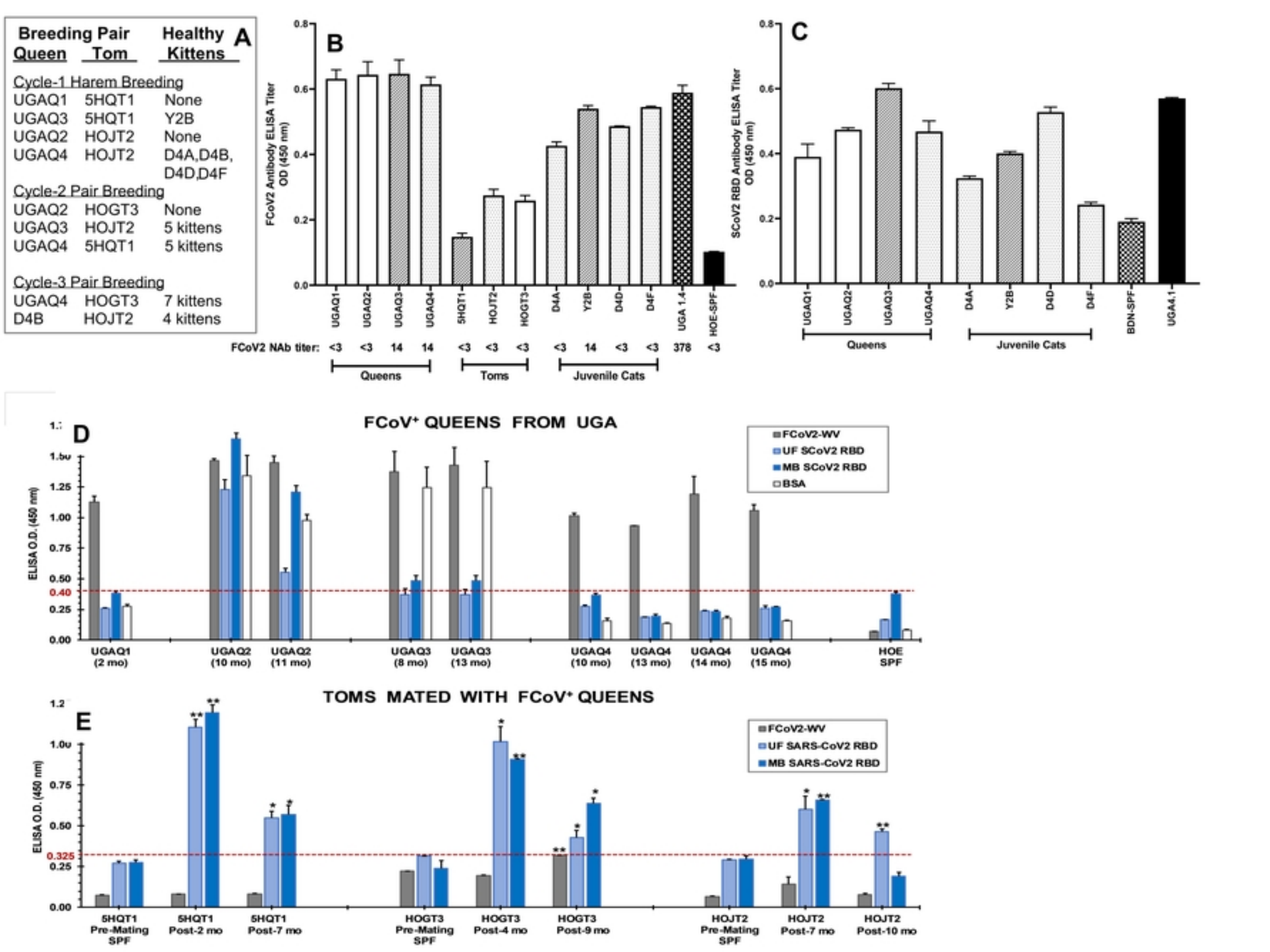
A
Breeding Pair
Queen Tom
Healthy Kittens
Cycle-1 Harem Breeding
UGAQ1 5HQT1 None
UGAQ3 5HQT1 Y2B
UGAQ2 HOJT2 None
UGAQ4 HOJT2 D4A,D4B, D4D,D4F
Cycle-2 Pair Breeding
UGAQ2 HOGT3 None
UGAQ3 HOJT2 5 kittens
UGAQ4 5HQT1 5 kittens
Cycle-3 Pair Breeding
UGAQ4 HOGT3 7 kittens
D4B HOJT2 4 kittens
B
FCoV2 Antibody ELISA Titer OD (450 nm)
UGAQ1 UGAQ2 UGAQ3 UGAQ4 5HQT1 HOJT2 HOGT3 D4A Y2B D4D D4F UGA 1.4 HOE-SPF
FCoV2 NAb titer: <3 <3 14 14 <3 <3 <3 <3 14 <3 <3 378 <3
Queens
Toms
Juvenile Cats
C
SCoV2 RBD Antibody ELISA Titer OD (450 nm)
UGAQ1 UGAQ2 UGAQ3 UGAQ4 D4A Y2B D4D D4F BDN-SPF UGA4.1
Queens
Juvenile Cats
D
FCoV+ QUEENS FROM UGA
FCoV2-WV
UF SCoV2 RBD
MB SCoV2 RBD
BSA
ELISA O.D. (450 nm)
0.40
UGAQ1 (2 mo)
UGAQ2 (10 mo)
UGAQ2 (11 mo)
UGAQ3 (8 mo)
UGAQ3 (13 mo)
UGAQ4 (10 mo)
UGAQ4 (13 mo)
UGAQ4 (14 mo)
UGAQ4 (15 mo)
HOE SPF
E
TOMS MATED WITH FCoV+ QUEENS
FCoV2-WV
UF SARS-CoV2 RBD
MB SARS-CoV2 RBD
ELISA O.D. (450 nm)
0.325
5HQT1 Pre-Mating SPF
5HQT1 Post-2 mo
5HQT1 Post-7 mo
HOGT3 Pre-Mating SPF
HOGT3 Post-4 mo
HOGT3 Post-9 mo
HOJT2 Pre-Mating SPF
HOJT2 Post-7 mo
HOJT2 Post-10 mo

Fig 1

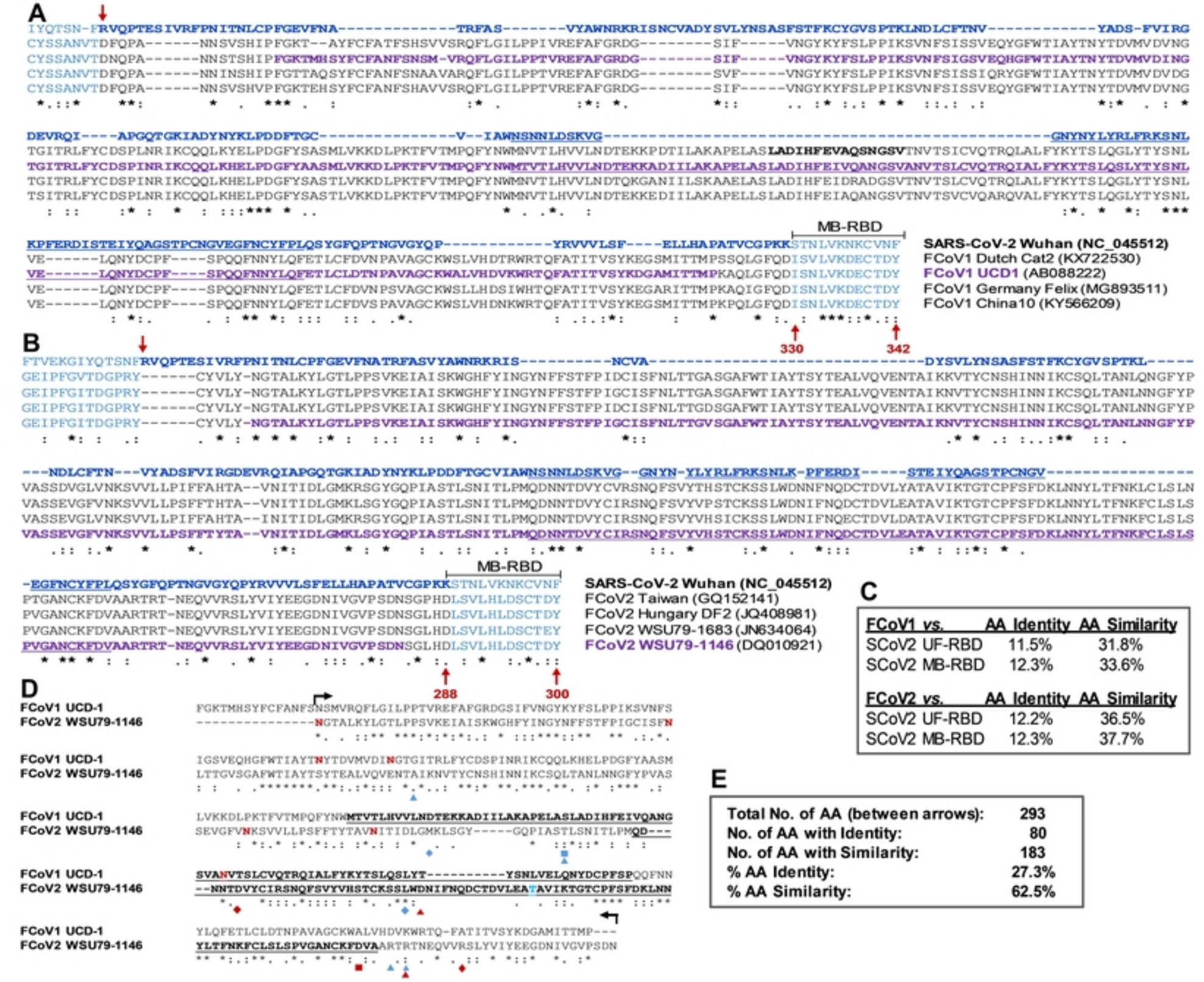
A
MB-RBD
SARS-CoV-2 Wuhan (NC_045512)
FCoV1 Dutch Cat2 (KX722530)
FCoV1 UCD1 (AB088222)
FCoV1 Germany Felix (MG893511)
FCoV1 China10 (KY566209)
330
342
B
MB-RBD
SARS-CoV-2 Wuhan (NC_045512)
FCoV2 Taiwan (GQ152141)
FCoV2 Hungary DF2 (JQ408981)
FCoV2 WSU79-1683 (JN634064)
FCoV2 WSU79-1146 (DQ010921)
288
300
C
FCoV1 vs. AA Identity AA Similarity
SCoV2 UF-RBD 11.5% 31.8%
SCoV2 MB-RBD 12.3% 33.6%
FCoV2 vs. AA Identity AA Similarity
SCoV2 UF-RBD 12.2% 36.5%
SCoV2 MB-RBD 12.3% 37.7%
D
FCoV1 UCD-1
FCoV2 WSU79-1146
E
Total No. of AA (between arrows): 293
No. of AA with Identity: 80
No. of AA with Similarity: 183
% AA Identity: 27.3%
% AA Similarity: 62.5%

Fig 2

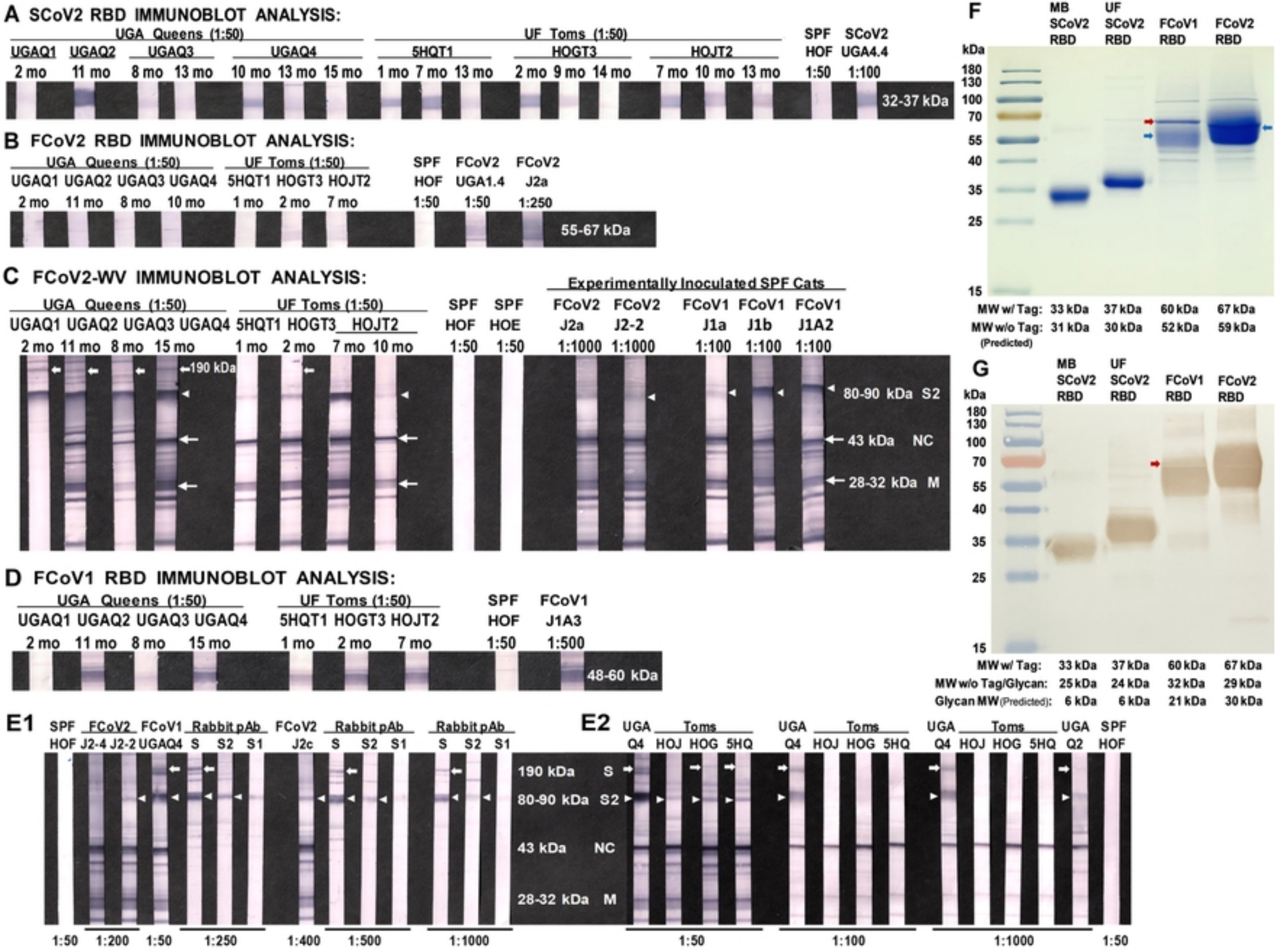
A SCoV2 RBD IMMUNOBLOT ANALYSIS:
UGA Queens (1:50)
UGAQ1 UGAQ2 UGAQ3 UGAQ4
2 mo 11 mo 8 mo 13 mo 10 mo 13 mo 15 mo
UF Toms (1:50)
5HQT1 HOGT3 HOJT2
1 mo 7 mo 13 mo 2 mo 9 mo 14 mo 7 mo 10 mo 13 mo
SPF HOF 1:50
SCoV2 UGA4.4 1:100
32-37 kDa
B FCoV2 RBD IMMUNOBLOT ANALYSIS:
UGA Queens (1:50)
UGAQ1 UGAQ2 UGAQ3 UGAQ4
2 mo 11 mo 8 mo 10 mo
UF Toms (1:50)
5HQT1 HOGT3 HOJT2
1 mo 2 mo 7 mo
SPF HOF 1:50
FCoV2 UGA1.4 1:50
FCoV2 J2a 1:250
55-67 kDa
C FCoV2-WV IMMUNOBLOT ANALYSIS:
Experimentally Inoculated SPF Cats
UGA Queens (1:50)
UGAQ1 UGAQ2 UGAQ3 UGAQ4
2 mo 11 mo 8 mo 15 mo
UF Toms (1:50)
5HQT1 HOGT3 HOJT2
1 mo 2 mo 7 mo 10 mo
SPF HOF 1:50
SPF HOE 1:50
FCoV2 J2a 1:1000
FCoV2 J2-2 1:1000
FCoV1 J1a 1:100
FCoV1 J1b 1:100
FCoV1 J1A2 1:100
190 kDa
80-90 kDa S2
43 kDa NC
28-32 kDa M
D FCoV1 RBD IMMUNOBLOT ANALYSIS:
UGA Queens (1:50)
UGAQ1 UGAQ2 UGAQ3 UGAQ4
2 mo 11 mo 8 mo 15 mo
UF Toms (1:50)
5HQT1 HOGT3 HOJT2
1 mo 2 mo 7 mo
SPF HOF 1:50
FCoV1 J1A3 1:500
48-60 kDa
E1
SPF HOF
FCoV2 J2-4 J2-2
FCoV1 UGAQ4
Rabbit pAb S S2 S1
FCoV2 J2c
Rabbit pAb S S2 S1
Rabbit pAb S S2 S1
190 kDa S
80-90 kDa S2
43 kDa NC
28-32 kDa M
1:50 1:200 1:50 1:250 1:400 1:500 1:1000
E2
UGA Q4
Toms HOJ HOG 5HQ
UGA Q4
Toms HOJ HOG 5HQ
UGA Q4
Toms HOJ HOG 5HQ
UGA Q2
SPF HOF
1:50 1:100 1:1000 1:50
F
MB SCoV2 RBD
UF SCoV2 RBD
FCoV1 RBD
FCoV2 RBD
kDa
180 130 100 70 55 40 35 25 15
MW w/ Tag: 33 kDa 37 kDa 60 kDa 67 kDa
MW w/o Tag: 31 kDa 30 kDa 52 kDa 59 kDa
(Predicted)
G
MB SCoV2 RBD
UF SCoV2 RBD
FCoV1 RBD
FCoV2 RBD
kDa
180 130 100 70 55 40 35 25 15
MW w/ Tag: 33 kDa 37 kDa 60 kDa 67 kDa
MW w/o Tag/Glycan: 25 kDa 24 kDa 32 kDa 29 kDa
Glycan MW (Predicted): 6 kDa 6 kDa 21 kDa 30 kDa

Fig 3

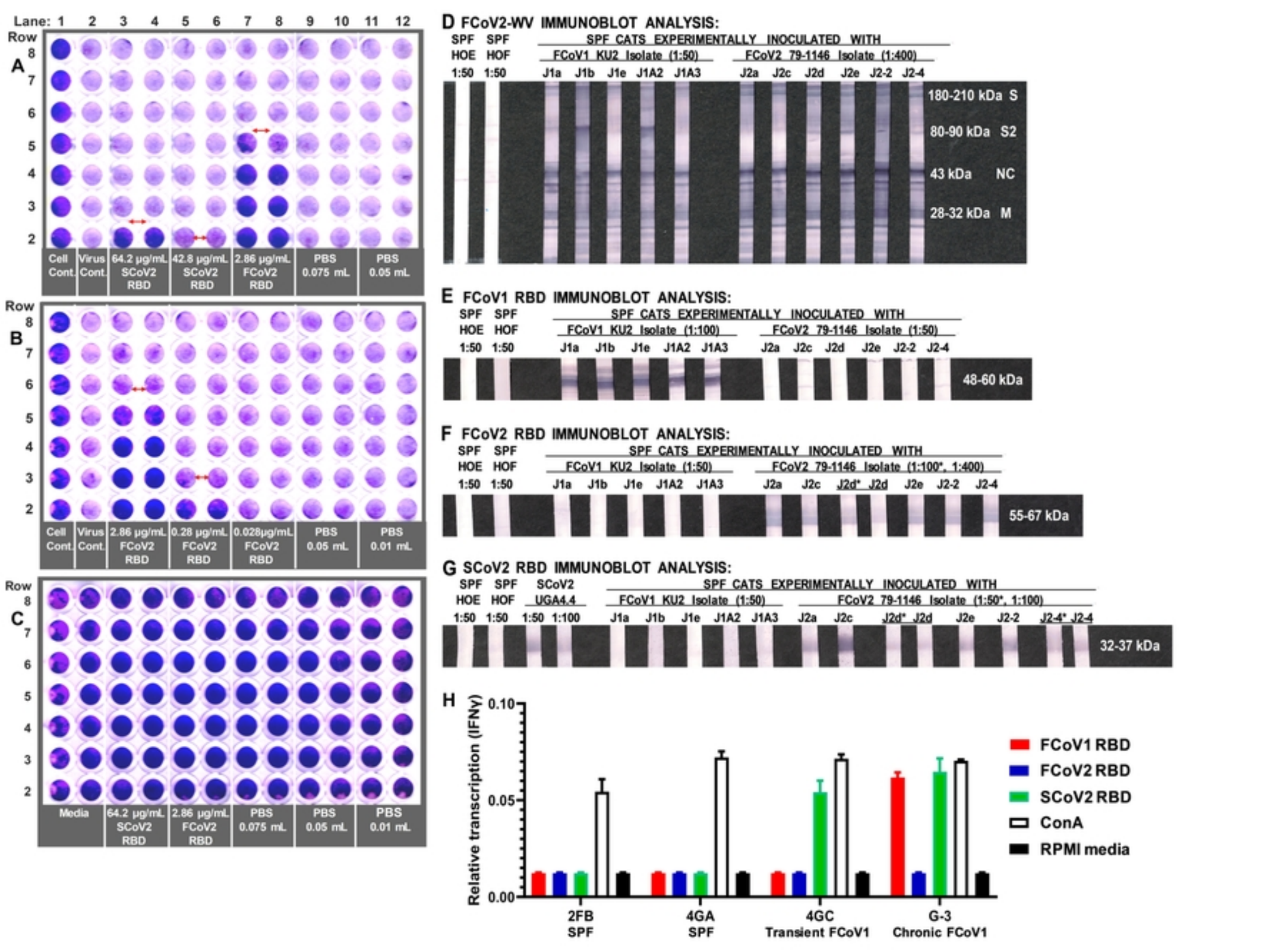
Lane: 1 2 3 4 5 6 7 8 9 10 11 12
Row
A
B
C
Cell Cont.
Virus Cont.
64.2 µg/mL SCoV2 RBD
42.8 µg/mL SCoV2 RBD
2.86 µg/mL FCoV2 RBD
PBS 0.075 mL
PBS 0.05 mL
2.86 µg/mL FCoV2 RBD
0.28 µg/mL FCoV2 RBD
0.028µg/mL FCoV2 RBD
PBS 0.01 mL
Media
D FCoV2-WV IMMUNOBLOT ANALYSIS:
SPF HOE 1:50
SPF HOE 1:50
SPF CATS EXPERIMENTALLY INOCULATED WITH
FCoV1 KU2 Isolate (1:50)
FCoV2 79-1146 Isolate (1:400)
J1a J1b J1e J1A2 J1A3 J2a J2c J2d J2e J2-2 J2-4
180-210 kDa S
80-90 kDa S2
43 kDa NC
28-32 kDa M
E FCoV1 RBD IMMUNOBLOT ANALYSIS:
FCoV1 KU2 Isolate (1:100)
FCoV2 79-1146 Isolate (1:50)
48-60 kDa
F FCoV2 RBD IMMUNOBLOT ANALYSIS:
FCoV1 KU2 Isolate (1:50)
FCoV2 79-1146 Isolate (1:100*, 1:400)
J2d* J2d
55-67 kDa
G SCoV2 RBD IMMUNOBLOT ANALYSIS:
SCoV2 UGA4.4
1:50 1:50 1:50 1:100
FCoV1 KU2 Isolate (1:50)
FCoV2 79-1146 Isolate (1:50*, 1:100)
J2-4* J2-4
32-37 kDa
H
Relative transcription (IFNγ)
0.10
0.05
0.00
2FB SPF
4GA SPF
4GC Transient FCoV1
G-3 Chronic FCoV1
FCoV1 RBD
FCoV2 RBD
SCoV2 RBD
ConA
RPMI media

Fig 4